

Article

# Radiative Transition Parameters in Atomic Lanthanum from Pseudo-Relativistic Hartree–Fock and Fully Relativistic Dirac–Hartree–Fock Calculations

Sébastien Gamrath <sup>1</sup>, Patrick Palmeri <sup>1</sup> and Pascal Quinet <sup>1,2,\*</sup>

<sup>1</sup> Physique Atomique et Astrophysique, Université de Mons, B-7000 Mons, Belgium; Sebastien.Gamrath@umons.ac.be (S.G.); Patrick.Palmeri@umons.ac.be (P.P.)

<sup>2</sup> IPNAS, Université de Liège, B-4000 Liège, Belgium

\* Correspondence: Pascal.Quinet@umons.ac.be; Tel.: +32-65-373629

Received: 23 January 2019; Accepted: 16 March 2019; Published: 20 March 2019



**Abstract:** Calculated radiative transition probabilities and oscillator strengths are reported for 392 lines of neutral lanthanum (La I) atom in the spectral range from the near ultraviolet to the mid infrared. They were obtained using two different theoretical methods based on the pseudo-relativistic Hartree–Fock (HFR) and the fully relativistic multiconfiguration Dirac–Hartree–Fock (MCDHF) approaches, both including the most important intravalence and core-valence electron correlations. The quality of these radiative parameters was assessed through detailed comparisons between the results obtained using different physical models and between our theoretical results and the experimental data, where available. Of the total number of La I lines listed in the present work, about 60% have *gf*- and *gA*-values determined for the first time.

**Keywords:** atomic structure; oscillator strengths; transition probabilities; La I spectrum

## 1. Introduction

The determination of radiative parameters in lanthanide atoms and ions has been the subject of many experimental and theoretical studies over the past few decades. This is mainly due to the fact that the remarkably rich spectra corresponding to the first ionization stages of these elements provide useful information for the development of other scientific fields, such as astrophysics and the lighting industry, as mentioned in numerous papers (see e.g., [1–5]).

Neutral lanthanum, La I ( $Z = 57$ ), is characterized by the  $5d6s^2D_{3/2}$  ground level, while, the lowest excited levels belong to many different configurations such as  $5d6s^2$ ,  $5d^26s$ ,  $5d^3$ ,  $4f6s6p$ ,  $5d^27s$ ,  $5d6s7s$ , for the even parity, and  $5d6s6p$ ,  $5d^26p$ ,  $4f5d6s$ ,  $6s^26p$ ,  $4f6s^2$ , for the odd parity, according to the National Institute of Standards and Technology (NIST) database [6]. The overlap of these configurations is responsible for the strong mixing of most energy levels, which makes both experimental and theoretical analyses very difficult. This notably explains why the designation of some low-lying La I levels is still uncertain or even not yet assigned.

The first measurements of transition probabilities in La I were published by Corliss and Bozman [7] more than 55 years ago. These data, which are known to be of limited accuracy, were after all taken on by Kurucz in his database [8]. During the 1970s and 1980s, radiative lifetimes were obtained for a few levels using different experimental methods, i.e., the level-crossing and double resonance [9–11], the laser-induced fluorescence [12], and the pulse-electron delayed coincidence [13] techniques. More recently, radiative lifetime measurements were performed with the time-resolved laser-induced fluorescence technique for 20 odd-parity levels of La I between 18,172 and 28,506  $\text{cm}^{-1}$  [14]. These

results were compared with pseudo-relativistic Hartree–Fock (HFR) calculations and, although the agreement of theory with experiment was generally satisfactory, large discrepancies were found for some levels, emphasizing the difficulty to get a reliable theoretical model in such a heavy and complex neutral element. Theoretical lifetimes, transition probabilities and oscillator strengths in La I were also obtained by Karaçoban and Özdemir [15,16] who used the multiconfiguration Hartree–Fock (MCHF) method within the framework of Breit–Pauli relativistic corrections [17]. Finally, the laser-induced fluorescence (LIF) technique was used to measure, with an estimated accuracy of 5–10%, the radiative lifetimes for 32 levels in the range 23,874–37,982  $\text{cm}^{-1}$  [18], 24 levels in the range 34,213–40,910  $\text{cm}^{-1}$  [19], 63 levels in the range 13,260–30,965  $\text{cm}^{-1}$  [20], 40 levels in the range 24,507–52,030  $\text{cm}^{-1}$  [21], and 72 levels in the range 15,031–32,140  $\text{cm}^{-1}$  [22]. The latter work was completed by Fourier transform spectroscopy measurements of branching fractions, which were combined with the experimental radiative lifetimes to yield transition probabilities for 315 lines in La I. This offers us a unique opportunity to test the reliability of new extensive theoretical models.

In the present paper, we report on moderately large-scale calculations of radiative decay rates in neutral lanthanum atom using two different methods, i.e., the pseudo-relativistic Hartree–Fock (HFR) and the fully relativistic multiconfiguration Dirac–Hartree–Fock (MCDHF) approaches. In both of them, the most important intravalence and core-valence electron interactions were considered. This allowed us to provide a set of oscillator strengths and transition probabilities for 392 strong La I spectral lines, in the wavelength range from 317 to 7843 nm, of which about 60% are given for the first time. The accuracy of these new radiative parameters was assessed through detailed comparisons between the results obtained in the present work using different physical models and between our theoretical results and the available experimental data.

## 2. Computational Methods Used

### 2.1. Pseudo-Relativistic Hartree–Fock Calculations

The first computational procedure used in the present work for modelling the atomic structure and calculating the radiative parameters in La I was the pseudo-relativistic Hartree–Fock (HFR) method, originally introduced by Cowan [23] and modified for taking core-polarization (CPOL) effects into account, giving rise to the so-called HFR+CPOL method [24–26]. Three different physical models were employed in the calculations.

In the first model (HFR-NOPOL), only intravalence correlation was considered by explicitly including the following 37 even- and 37 odd-parity configurations, namely  $5d6s^2$ ,  $5d^26s$ ,  $5d^27s$ ,  $5d^26d$ ,  $5d^3$ ,  $5d6p^2$ ,  $5d6d^2$ ,  $5d7s^2$ ,  $5d6s6d$ ,  $5d6s7s$ ,  $5d6p7p$ ,  $5d6d7s$ ,  $4f^25d$ ,  $4f^26d$ ,  $4f^26s$ ,  $4f^27s$ ,  $4f5d6p$ ,  $4f5d7p$ ,  $4f6s6p$ ,  $4f6s7p$ ,  $4f6p6d$ ,  $4f6p7s$ ,  $4f6d7p$ ,  $4f7s7p$ ,  $6s^26d$ ,  $6s^27s$ ,  $6s6p^2$ ,  $6s6d^2$ ,  $6s7s^2$ ,  $6s6p7p$ ,  $6s6d7s$ ,  $6p^26d$ ,  $6p^27s$ ,  $6p6d7p$ ,  $6p7s7p$ ,  $6d7s^2$ ,  $7s6d^2$ , and  $5d^26p$ ,  $5d^27p$ ,  $5d6s6p$ ,  $5d6s7p$ ,  $5d6p6d$ ,  $5d6p7s$ ,  $5d6d7p$ ,  $5d7s7p$ ,  $4f^3$ ,  $4f^26p$ ,  $4f^27p$ ,  $4f5d^2$ ,  $4f6s^2$ ,  $4f6p^2$ ,  $4f6d^2$ ,  $4f7s^2$ ,  $4f5d6s$ ,  $4f5d7s$ ,  $4f5d6d$ ,  $4f6s6d$ ,  $4f6s7s$ ,  $4f6p7p$ ,  $4f6d7s$ ,  $6s^26p$ ,  $6s^27p1$ ,  $6s6p6d$ ,  $6s6p7s$ ,  $6s6d7p$ ,  $6s7s7p$ ,  $6p^3$ ,  $6p^27p$ ,  $6p6d^2$ ,  $6p7s^2$ ,  $6p6d7s$ ,  $6d^27p$ ,  $6d7s7p$ ,  $7s^27p$ , respectively. It is worth noting that these multiconfiguration expansions are considerably more extensive than those included in our previous HFR calculations published 15 years ago [14].

In the second model (HFR+CPOL1), the same set of configurations as the one given hereabove was explicitly considered in the computations. In addition, core-polarization effects were estimated by assuming a Xe-like La IV ionic core with the dipole polarizability value reported by Fraga et al. [27], i.e.,  $\alpha_d = 9.50 a_0^3$ , and a cut-off radius equal to the HFR average value  $\langle r \rangle$  of the outermost core orbital (5p), i.e.,  $r_c = 1.80 a_0$ .

However, as mentioned, for example, in [28], the cut-off radius is not an unambiguously defined parameter. Therefore, the core-polarization contributions were also estimated in a third model (HFR+CPOL2), in which we used the same dipole polarizability as the one used in HFR+CPOL1 but with a different value of the cut-off radius, namely  $r_c = 1.20 a_0$ , representing the distance at which the total probability density of the ionic core orbitals falls to 10 per cent of its maximum value,

as suggested in [29]. This is illustrated in Figure 1 which shows the calculated probability density of the La IV ionic core in the ground configuration of the lanthanum atom.

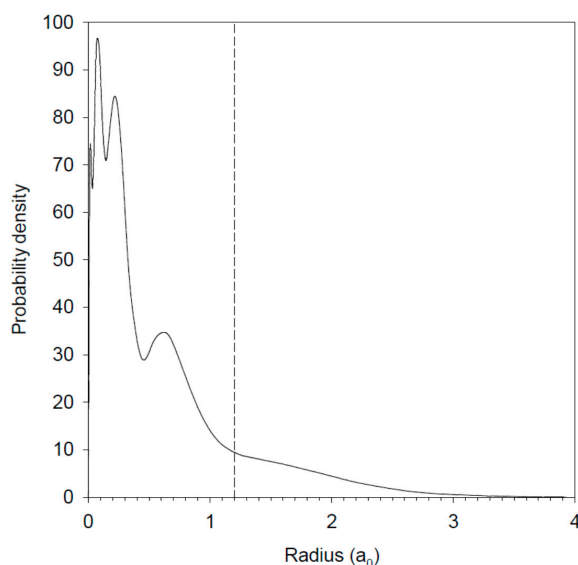


**Figure 1.** Electron probability density ( $P_{nl}^2$ ) of the La IV ionic core in the ground configuration ( $5d6s^2$ ) of neutral lanthanum. The value of the cut-off radius used in the HFR+CPOL2 calculations ( $r_c = 1.20 a_0$ ) is also shown in the figure. It represents the distance at which the electron probability density falls to 10 percent of its maximum value, as suggested in [29].

Furthermore, in each of these three models, the calculated eigenvalues of the Hamiltonian were optimized to the observed energy levels via a well-established least-squares fitting procedure [23] in which all the experimentally known levels included in the NIST compilation [6] up to  $32,140 \text{ cm}^{-1}$  were included, most of the level values above that limit being affected by dubious or unknown assignments. It is worth mentioning that the newly identified even-parity level at  $25,558.774 \text{ cm}^{-1}$  ( $J = 3/2$ ) [30] was also incorporated in the fitting process. For this level, the leading component (52%) was found to be  $5d^3^2D_{3/2}$ , according to our calculations. In this semi-empirical procedure, some radial energy parameters, such as the average energies, Slater integrals, spin-orbit parameters and effective interaction parameters, characterizing the  $5d6s^2$ ,  $5d^26s$ ,  $5d^27s$ ,  $5d^26d$ ,  $5d^3$ ,  $5d6s7s$ ,  $4f6s6p$  even-parity configurations, and the  $5d^26p$ ,  $5d6s6p$ ,  $4f6s^2$ ,  $4f5d6s$ ,  $6s^26p$  odd-parity configurations, were adjusted, giving rise to standard deviations of  $129 \text{ cm}^{-1}$  and  $173 \text{ cm}^{-1}$  for even and odd parities, respectively, whether for HFR-NOPOL, HFR+CPOL1 or HFR+CPOL2 models.

## 2.2. Fully Relativistic Multiconfiguration Dirac–Hartree–Fock Calculations

In order to assess the reliability of the pseudo-relativistic Hartree–Fock computations described above, another theoretical method used in our work was the one implemented in the GRASP2K computer package [31] which uses the fully relativistic multiconfiguration Dirac–Hartree–Fock (MCDHF) method [32].

In a first step, the  $5d6s^2$ ,  $5d^26s$ ,  $5d^27s$ ,  $5d^26d$ ,  $5d^3$ ,  $5d6s7s$ ,  $4f6s6p$  even-parity configurations, and the  $5d^26p$ ,  $5d^27p$ ,  $5d6s6p$ ,  $5d6s7p$ ,  $6s^26p$ ,  $6s^27p$ ,  $4f5d^2$ ,  $4f6s^2$  odd-parity configurations were chosen as multireference to optimize all the involved orbitals using the extended average level (EAL) option [31]. The valence-valence correlations were then taken into account by allowing single and double excitations from the multireference to  $5d$ ,  $5f$ ,  $5g$ ,  $6s$ ,  $6p$ ,  $6d$ ,  $7s$ ,  $7p$ ,  $7d$ ,  $8s$ ,  $8p$  and  $8d$  orbitals, giving rise to 20,265 CSFs. In this step, the additional  $5f$ ,  $5g$ ,  $7d$ ,  $8s$ ,  $8p$  and  $8d$  orbitals were first obtained by an EAL variational procedure, keeping frozen all the other orbitals, before re-optimizing all the orbitals together. Finally, the most important core-valence correlations were considered by including the  $5p \rightarrow 4f$ ,  $5s \rightarrow 5d$  single excitations, and the  $5p^2 \rightarrow 5d^2$ ,  $5s^2 \rightarrow 4f^2$ ,  $5s5p \rightarrow 4f5d$  double

excitations within the relativistic configuration interaction (RCI) approximation. This led to a total number of 84,314 CSFs. In addition, higher-order relativistic effects, such as the transverse-photon Breit interaction, together with the leading quantum electrodynamics (QED) corrections due to self-energy and vacuum polarization effects [32], were also incorporated in the calculations.

### 3. Results and Discussion

#### 3.1. Radiative Lifetimes

In Table 1, the calculated lifetime values, obtained using our three different HFR models, are compared with the available measurements performed by time-resolved laser-induced fluorescence spectroscopy (TR-LIF) for 96 odd-parity levels in La I. We note that the theoretical results are in satisfactory agreement with the most recent and the most accurate experimental data of Den Hartog et al. [22], if we except the three levels at 17,947.13, 23,221.10 and 24,173.83  $\text{cm}^{-1}$  for which large discrepancies, exceeding a factor of 3, are observed. This can be explained by the poor representation of these levels in our theoretical models, as evidenced by the rather bad agreement we found when comparing the calculated HFR Landé  $g$ -factors, i.e.,  $g \sim 1.06, 1.08, \text{ and } 0.72$ , with the experimental values [6], i.e.,  $g = 1.516, 0.781, \text{ and } 0.806$ , respectively. It is interesting to notice however that, for the level at 24,173.83  $\text{cm}^{-1}$ , the lifetime computed by Karaçoban and Özdemir [15], i.e.,  $\delta = 6.04 \text{ ns}$ , is in better agreement with our values (ranging from 9.6 to 12.0 ns) than with the experimental one (35.9 ns). When looking into more details, and when excluding the three levels mentioned above from the comparison, the mean ratios are found to be  $\delta(\text{HFR-NOPOL})/\delta(\text{EXP [22]}) = 0.77 \pm 0.18$ ,  $\delta(\text{HFR+CPOL1})/\delta(\text{EXP [22]}) = 0.90 \pm 0.23$ , and  $\delta(\text{HFR+CPOL2})/\delta(\text{EXP [22]}) = 0.94 \pm 0.22$ , where the uncertainty corresponds to the standard deviation from the average. Firstly, as expected, it is clear that the core-valence correlations play a non-negligible role, the calculated lifetimes increasing by about 15% when including core-polarization contributions. Secondly, it appears that the HFR+CPOL2 model gives the best overall agreement with the experimental radiative lifetimes [22]. This agreement is also better than the one obtained when comparing the theoretical lifetimes calculated by Biémont et al. [14] (for 17 levels) and by Karaçoban and Özdemir [15] (for 37 levels) to the experimental measurements. Indeed, in these two cases, the mean ratios  $\delta(\text{THEORY})/\delta(\text{EXP [22]})$  are found to be equal to  $0.98 \pm 0.33$  and  $0.89 \pm 0.47$ , respectively, the standard deviations (and therefore the scattering of results) being larger than the value obtained when using the HFR+CPOL2 model of the present work, which can thus be considered as the most reliable one. The comparison between the radiative lifetimes computed with the latter model and the TR-LIF experimental data of [22] is illustrated in Figure 2.

Some other laser-induced fluorescence lifetime measurements were published before the work of Den Hartog et al. [22]. These data [14,18,20,21] are also reported in Table 1. The comparison between our HFR+CPOL2 calculated values with the latter gives the mean ratios  $\delta(\text{HFR+CPOL2})/\delta(\text{EXP [14]}) = 0.81 \pm 0.20$ ,  $\delta(\text{HFR+CPOL2})/\delta(\text{EXP [18]}) = 0.93 \pm 0.24$ ,  $\delta(\text{HFR+CPOL2})/\delta(\text{EXP [20]}) = 0.91 \pm 0.43$ , and  $\delta(\text{HFR+CPOL2})/\delta(\text{EXP [21]}) = 0.88 \pm 0.20$ , the larger scattering observed when using the experimental data of Yarlagadda et al. [20] being mainly due to the fact that many of the levels considered by these authors have rather long lifetimes ( $\delta > 100 \text{ ns}$ ), which are more difficult to precisely determine both experimentally and theoretically.

Finally, let us note that the MCDHF lifetimes calculated in the present work are not listed in Table 1 because, for many levels (about 50%), either the identifications are rather difficult to unambiguously establish in the calculations (in particular for  $E > 26,000 \text{ cm}^{-1}$ ), or most of the computed radiative decay rates are strongly affected by severe cancellation effects leading to very uncertain lifetimes (in particular for  $\delta > 100 \text{ ns}$ ). It is useful to remind here that we have recently modified [33] the GRASP2K package to include the calculation of the cancellation factor (CF) as defined by Cowan [23]. Nevertheless, for clearly identified levels in our MCDHF calculations, it is interesting to point out that the theoretical lifetimes are generally slightly shorter than the experimental data of Den Hartog et al. [22], just like when compared to our HFR+CPOL2 results, the mean ratios being found to

be  $\hat{\omega}(\text{MCDHF})/\hat{\omega}(\text{EXP [22]}) = 0.85 \pm 0.46$  and  $\hat{\omega}(\text{MCDHF})/\hat{\omega}(\text{HFR+CPOL2}) = 0.81 \pm 0.43$ , respectively. This can be explained by the fact that core-valence interactions are taken into account more effectively by using the core-polarization corrections in the HFR method than by explicitly incorporating a limited set of core-excited configurations in the MCDHF model.

**Table 1.** Comparison of the radiative lifetimes computed in the present work using three different HFR models with the most recent available experimental values for odd-parity levels in La I.

E (cm <sup>-1</sup> )	Level <sup>a</sup> Designation	J	This Work (ns) <sup>b</sup>			Experiment (ns)	
			HFR-NOPOL	HFR+CPOL1	HFR+CPOL2	DH2015 <sup>c</sup>	Previous
13,260.38	5d6s(3D)6p 4F <sup>o</sup>	1.5	232	287	335		256.9 ± 12.3 <sup>f</sup>
13,631.04	5d6s(3D)6p ? <sup>o</sup>	2.5	213	260	295		224.5 ± 13.8 <sup>f</sup>
14,095.69	5d6s(3D)6p 4D <sup>o</sup>	0.5	119	149	179		220.9 ± 14.3 <sup>f</sup>
14,708.92	5d6s(3D)6p 4D <sup>o</sup>	1.5	158	198	239		166.3 ± 9.3 <sup>f</sup>
14,804.08	5d6s(3D)6p 4F <sup>o</sup>	2.5	194	236	270		257.9 ± 21.5 <sup>f</sup>
15,019.51	5d6s(3D)6p 4F <sup>o</sup>	3.5	247	305	357		313.0 ± 17.8 <sup>f</sup>
15,031.64	5d6s(3D)6p ? <sup>o</sup>	1.5	155	192	224	162 ± 8	183.7 ± 12.8 <sup>f</sup>
15,196.83	4f6s <sup>2</sup> 2F <sup>o</sup>	2.5	106	123	132	108 ± 5	127.0 ± 7.0 <sup>f</sup>
15,219.89	5d6s(3D)6p ? <sup>o</sup>	0.5	355	459	585		205.4 ± 16.9 <sup>f</sup>
15,503.64	5d6s(3D)6p 4D <sup>o</sup>	2.5	106	132	158		131.8 ± 6.8 <sup>f</sup>
16,099.29	5d6s(3D)6p 4D <sup>o</sup>	3.5	102	127	153		156.7 ± 14.2 <sup>f</sup>
16,280.26	6s <sup>2</sup> 6p ? <sup>o</sup>	1.5	211	269	337		271.6 ± 19.2 <sup>f</sup>
16,538.39	4f6s <sup>2</sup> 2F <sup>o</sup>	3.5	68.1	78.8	83.7	85.3 ± 4.3	112.9 ± 9.5 <sup>f</sup>
16,856.80	5d <sup>2</sup> (3F)6p ? <sup>o</sup>	2.5	34.6	40.6	42.2	52.4 ± 2.6	68.4 ± 5.1 <sup>f</sup>
17,797.29	5d6s(3D)6p 4P <sup>o</sup>	1.5	236	287	341		130.2 ± 11.5 <sup>f</sup>
17,910.17	5d <sup>2</sup> (3F)6p ? <sup>o</sup>	3.5	44.4	52.0	54.5	48.9 ± 2.4	64.6 ± 2.7 <sup>f</sup>
17,947.13	5d <sup>2</sup> (3F)6p 4G <sup>o</sup>	2.5	115	138	154	51.4 ± 2.6	68.3 ± 3.1 <sup>f</sup>
18,156.97	5d6s(3D)6p 4P <sup>o</sup>	2.5	28.4	33.1	34.5	64.0 ± 3.2	68.4 ± 3.1 <sup>f</sup>
18,172.35	5d <sup>2</sup> (3F)6p 2D <sup>o</sup>	1.5	10.7	12.7	13.3	15.7 ± 0.8	17.7 ± 1.4 <sup>d</sup>
18,603.92	5d <sup>2</sup> (3F)6p 4G <sup>o</sup>	3.5	27.5	31.8	33.1	37.6 ± 1.9	54.8 ± 3.5 <sup>f</sup>
19,129.31	5d <sup>2</sup> (3F)6p 4G <sup>o</sup>	4.5	21.7	25.0	25.9	29.4 ± 1.5	46.0 ± 2.6 <sup>f</sup>
19,379.40	5d <sup>2</sup> (3F)6p 2D <sup>o</sup>	2.5	10.3	12.2	12.8	15.3 ± 0.8	17.2 ± 1.0 <sup>d</sup>
							15.9 ± 1.0 <sup>f</sup>
20,018.99	5d6s(1D)6p ? <sup>o</sup>	1.5	11.2	13.2	13.9	14.1 ± 0.7	17.0 ± 0.8 <sup>f</sup>
20,082.98	5d <sup>2</sup> (3F)6p 4F <sup>o</sup>	1.5	14.2	16.4	17.1	15.1 ± 0.8	17.5 ± 1.6 <sup>f</sup>
20,117.38	5d <sup>2</sup> (3F)6p 4G <sup>o</sup>	5.5	20.6	23.7	24.6	27.2 ± 1.4	32.0 ± 2.2 <sup>f</sup>
20,197.34	5d6s(1D)6p ? <sup>o</sup>	0.5	8.4	9.9	10.5	9.8 ± 0.5	17.2 ± 0.8 <sup>f</sup>
20,338.25	5d <sup>2</sup> (3F)6p 4F <sup>o</sup>	2.5	15.1	17.5	18.3	18.7 ± 0.9	20.0 ± 0.9 <sup>f</sup>
20,763.21	5d <sup>2</sup> (3F)6p 4F <sup>o</sup>	3.5	15.2	17.6	18.3	20.4 ± 1.0	25.8 ± 1.4 <sup>f</sup>
20,972.17	5d <sup>2</sup> (3F)6p ? <sup>o</sup>	2.5	17.9	21.0	22.1	25.7 ± 1.3	35.0 ± 3.5 <sup>f</sup>
21,384.00	5d <sup>2</sup> (3F)6p 4F <sup>o</sup>	4.5	14.6	17.0	17.7	19.9 ± 1.0	23.0 ± 2.1 <sup>f</sup>
21,447.86	5d <sup>2</sup> (3F)6p ? <sup>o</sup>	3.5	26.0	30.0	31.4	29.2 ± 1.5	34.1 ± 3.3 <sup>f</sup>
21,662.51	5d <sup>2</sup> (3F)6p 2G <sup>o</sup>	3.5	20.4	23.8	25.0	32.1 ± 1.6	39.8 ± 2.1 <sup>f</sup>
22,246.64	5d <sup>2</sup> (3F)6p 4D <sup>o</sup>	0.5	6.7	7.9	8.3	8.6 ± 0.4	10.1 ± 0.9 <sup>d</sup>
							9.6 ± 0.6 <sup>f</sup>
22,285.77	5d <sup>2</sup> (3F)6p 2G <sup>o</sup>	4.5	47.0	53.5	56.1	51.8 ± 2.6	73.4 ± 6.1 <sup>f</sup>
22,439.36	5d <sup>2</sup> (3F)6p 4D <sup>o</sup>	1.5	6.6	7.7	8.2	8.8 ± 0.4	10.2 ± 0.5 <sup>d</sup>
							9.5 ± 0.7 <sup>f</sup>
22,804.25	5d <sup>2</sup> (3F)6p 4D <sup>o</sup>	2.5	6.6	7.7	8.1	8.9 ± 0.4	10.7 ± 1.0 <sup>d</sup>
							10.4 ± 0.3 <sup>f</sup>
23,221.10	5d6s(3D)6p ? <sup>o</sup>	3.5	109	127	134	21.1 ± 1.1	22.0 ± 1.4 <sup>d</sup>
							27.5 ± 2.7 <sup>f</sup>
23,260.92	5d <sup>2</sup> (3P)6p 2S <sup>o</sup>	0.5	13.6	16.0	17.0		18.1 ± 1.5 <sup>f</sup>
23,303.26	5d <sup>2</sup> (3P)6p 4D <sup>o</sup>	3.5	6.9	8.1	8.6	14.7 ± 0.7	16.1 ± 1.0 <sup>d</sup>
							16.5 ± 1.1 <sup>f</sup>
23,466.84	4f5d(1G <sup>o</sup> )6s 2G <sup>o</sup>	4.5	56.0	64.7	67.8	60.6 ± 3.0	67.9 ± 3.8 <sup>f</sup>
23,528.45	5d <sup>2</sup> (3P)6p 4D <sup>o</sup>	0.5	16.6	19.3	20.3	25.2 ± 1.3	27.8 ± 1.8 <sup>f</sup>
23,704.81	5d <sup>2</sup> (3P)6p 4D <sup>o</sup>	1.5	20.4	23.7	24.8	27.0 ± 1.4	31.2 ± 2.5 <sup>f</sup>
23,874.95	5d6s(3D)6p ? <sup>o</sup>	2.5	9.2	10.8	11.2	14.7 ± 0.7	16.2 ± 1.0 <sup>d</sup>
							14.7 ± 1.1 <sup>e</sup>
24,046.10	5d <sup>2</sup> (3P)6p 4D <sup>o</sup>	2.5	21.6	25.1	26.2	32.1 ± 1.6	16.1 ± 1.0 <sup>f</sup>
24,088.54	4f5d(1H <sup>o</sup> )6s 4H <sup>o</sup>	3.5	81.9	95.6	100.0		247 ± 12 <sup>e</sup>
							207.5 ± 14.5 <sup>f</sup>
24,173.83	4f5d(3F <sup>o</sup> )6s 4F <sup>o</sup>	1.5	9.6	11.4	12.0	35.9 ± 1.8	37.7 ± 1.4 <sup>f</sup>
24,409.68	4f5d(1G <sup>o</sup> )6s ? <sup>o</sup>	3.5	17.9	20.7	21.6	14.3 ± 0.7	15.7 ± 0.7 <sup>d</sup>
							14.6 ± 1.2 <sup>e</sup>
24,507.87	4f5d(3F <sup>o</sup> )6s 4F <sup>o</sup>	2.5	13.5	15.9	16.7	19.3 ± 1.0	21.9 ± 1.0 <sup>d</sup>
							19.2 ± 1.5 <sup>e</sup>
							22.2 ± 1.9 <sup>f</sup>
							20.0 ± 0.8 <sup>g</sup>

Table 1. Cont.

E (cm <sup>-1</sup> )	Level <sup>a</sup> Designation	J	This Work (ns) <sup>b</sup>			Experiment (ns)	
			HFR-NOPOLHFR+CPOL1	HFR+CPOL2	DH2015 <sup>c</sup>	Previous	
24,639.26	5d <sup>2</sup> ( <sup>3</sup> P)6p <sup>4</sup> S <sup>o</sup>	1.5	13.9	16.4	17.3	16.0 ± 0.8	14.9 ± 0.9 <sup>e</sup>
24,762.60	5d <sup>2</sup> ( <sup>3</sup> P)6p? <sup>2</sup> D <sup>o</sup> ?	1.5	11.3	13.2	13.7	10.6 ± 0.5	12.4 ± 1.1 <sup>f</sup>
24,910.38	4f5d( <sup>1</sup> D <sup>o</sup> )6s? ? <sup>o</sup>	1.5	16.8	19.4	20.3	30.6 ± 1.5	32.4 ± 1.8 <sup>f</sup>
24,984.29	5d <sup>2</sup> ( <sup>3</sup> P)6p? ? <sup>o</sup>	2.5	19.1	22.3	23.4	21.6 ± 1.1	27.2 ± 1.9 <sup>f</sup>
25,083.36	5d <sup>2</sup> ( <sup>3</sup> P)6p <sup>4</sup> D <sup>o</sup>	3.5	9.5	11.0	11.5	19.1 ± 1.0	21.1 ± 0.9 <sup>d</sup>
25,218.27	5d <sup>2</sup> ( <sup>3</sup> P)6p ? <sup>o</sup>	2.5	9.8	11.6	12.3	14.4 ± 0.7	15.7 ± 1.1 <sup>f</sup>
25,380.27	4f5d( <sup>3</sup> F <sup>o</sup> )6s <sup>4</sup> F <sup>o</sup>	3.5	13.2	15.6	16.4	21.4 ± 1.1	23.2 ± 1.3 <sup>d</sup>
25,453.95	5d6s( <sup>3</sup> D)6p ? <sup>o</sup>	0.5	6.6	7.8	8.4	9.6 ± 0.5	19.4 ± 0.8 <sup>f</sup>
25,616.95	5d <sup>2</sup> ( <sup>3</sup> P)6p <sup>4</sup> P <sup>o</sup>	0.5	15.3	17.7	18.5	17.8 ± 0.9	17.6 ± 1.1 <sup>e</sup>
25,643.00	5d <sup>2</sup> ( <sup>3</sup> P)6p <sup>4</sup> P <sup>o</sup>	1.5	18.7	21.7	22.8	13.7 ± 0.7	16.2 ± 0.8 <sup>f</sup>
25,874.52	5d <sup>2</sup> ( <sup>1</sup> G)6p ? <sup>o</sup>	5.5	46.4	53.0	55.4	61.7 ± 3.1	
25,950.32	5d <sup>2</sup> ( <sup>3</sup> P)6p ? <sup>o</sup>	1.5	7.6	8.9	9.5	11.9 ± 0.6	11.8 ± 0.9 <sup>e</sup>
25,997.17	4f5d( <sup>3</sup> F <sup>o</sup> )6s <sup>4</sup> F <sup>o</sup>	4.5	14.1	16.8	17.7	21.2 ± 1.1	23.3 ± 1.5 <sup>d</sup> 21.8 ± 0.9 <sup>f</sup> 21.6 ± 1.0 <sup>g</sup>
26,338.93	5d <sup>2</sup> ( <sup>3</sup> P)6p <sup>4</sup> P <sup>o</sup>	2.5	15.9	18.5	19.3	16.7 ± 0.8	16.5 ± 1.2 <sup>e</sup>
27,022.62	4f5d( <sup>3</sup> G <sup>o</sup> )6s <sup>4</sup> G <sup>o</sup>	2.5	13.7	16.3	16.8	19.5 ± 1.0	18.9 ± 1.4 <sup>e</sup> 20.9 ± 1.3 <sup>f</sup>
27,054.96	5d <sup>2</sup> ( <sup>1</sup> G)6p ? <sup>o</sup>	4.5	56.5	64.3	67.1		89.7 ± 4.4 <sup>g</sup>
27,132.44	5d <sup>2</sup> ( <sup>1</sup> G)6p <sup>2</sup> G <sup>o</sup>	3.5	13.5	15.9	16.8	16.4 ± 0.8	16.6 ± 1.2 <sup>e</sup>
27,225.26	5d <sup>2</sup> ( <sup>3</sup> P)6p <sup>2</sup> P <sup>o</sup>	1.5	9.3	10.8	11.4	15.4 ± 0.8	17.1 ± 0.9 <sup>d</sup>
27,393.04	5d <sup>2</sup> ( <sup>1</sup> D)6p ? <sup>o</sup>	2.5	13.1	15.6	16.2	12.4 ± 0.6	14.1 ± 0.6 <sup>d</sup> 12.6 ± 0.8 <sup>e</sup> 12.6 ± 0.6 <sup>g</sup>
27,455.31	4f5d( <sup>3</sup> G <sup>o</sup> )6s <sup>4</sup> G <sup>o</sup>	3.5	11.1	13.2	13.6	19.6 ± 1.0	21.6 ± 1.6 <sup>d</sup> 19.8 ± 1.4 <sup>e</sup>
27,619.54	5d <sup>2</sup> ( <sup>1</sup> G)6p <sup>2</sup> G <sup>o</sup>	4.5	10.9	12.7	13.4	12.7 ± 0.6	14.3 ± 1.1 <sup>e</sup>
27,669.37	4f5d( <sup>3</sup> F <sup>o</sup> )6s <sup>2</sup> F <sup>o</sup>	2.5	9.6	11.1	11.7	15.7 ± 0.8	17.8 ± 0.9 <sup>d</sup> 15.6 ± 0.7 <sup>g</sup>
27,748.97	5d <sup>2</sup> ( <sup>3</sup> P)6p <sup>2</sup> P <sup>o</sup>	0.5	10.7	12.6	13.3		27.0 ± 2.6 <sup>f</sup>
27,968.54	4f5d( <sup>3</sup> D <sup>o</sup> )6s ? <sup>o</sup>	1.5	8.6	9.6	10.5	6.5 ± 0.3	9.5 ± 0.9 <sup>f</sup>
28,039.45	5d6s( <sup>1</sup> D)6p ? <sup>o</sup>	3.5	10.4	12.4	12.9	11.9 ± 0.6	13.0 ± 0.9 <sup>d</sup> 11.9 ± 0.8 <sup>e</sup>
28,089.17	4f5d( <sup>3</sup> G <sup>o</sup> )6s <sup>4</sup> G <sup>o</sup>	4.5	11.5	13.8	14.0	18.5 ± 0.9	21.8 ± 1.8 <sup>f</sup>
28,506.41	5d6s( <sup>3</sup> D)6p ? <sup>o</sup>	2.5	6.2	7.1	7.5	8.0 ± 0.4	7.9 ± 0.3 <sup>d</sup> 7.9 ± 0.4 <sup>e</sup>
28,543.08	4f5d( <sup>3</sup> F <sup>o</sup> )6s <sup>2</sup> F <sup>o</sup>	3.5	13.1	15.2	15.9	20.1 ± 1.0	21.7 ± 1.2 <sup>d</sup> 19.7 ± 1.1 <sup>e</sup>
28,743.24	4f5d( <sup>3</sup> G <sup>o</sup> )6s <sup>4</sup> G <sup>o</sup>	5.5	10.9	13.1	13.2	17.8 ± 0.9	23.8 ± 1.6 <sup>f</sup>
28,893.51	4f5d( <sup>3</sup> D <sup>o</sup> )6s <sup>4</sup> D <sup>o</sup>	0.5	10.3	12.2	12.8		20.0 ± 1.7 <sup>f</sup>
28,971.84	4f5d( <sup>3</sup> D <sup>o</sup> )6s ? <sup>o</sup>	1.5	9.9	11.5	12.0		17.2 ± 1.2 <sup>f</sup>
29,199.57	4f5d( <sup>3</sup> D <sup>o</sup> )6s ? <sup>o</sup>	1.5	8.6	10.1	10.5		15.4 ± 0.8 <sup>e</sup>
29,466.67	[4f5d( <sup>3</sup> G <sup>o</sup> )6s <sup>2</sup> G <sup>o</sup> ]	3.5	12.2	14.2	14.7		28.3 ± 0.9 <sup>f</sup>
29,502.18	4f5d( <sup>3</sup> D <sup>o</sup> )6s ? <sup>o</sup>	2.5	11.6	13.4	14.2	11.2 ± 0.6	10.4 ± 0.9 <sup>e</sup>
29,564.70	4f5d( <sup>3</sup> P <sup>o</sup> )6s ? <sup>o</sup>	0.5	10.1	11.8	12.6		16.9 ± 0.8 <sup>g</sup>
29,775.58	4f5d( <sup>3</sup> D <sup>o</sup> )6s ? <sup>o</sup>	2.5	9.3	11.0	11.5	13.3 ± 0.7	12.3 ± 1.1 <sup>e</sup>
29,894.91	4f5d( <sup>3</sup> D <sup>o</sup> )6s ? <sup>o</sup>	3.5	10.3	12.2	12.6	15.6 ± 0.8	14.9 ± 0.8 <sup>e</sup>
29,936.74	4f5d( <sup>3</sup> P <sup>o</sup> )6s ? <sup>o</sup>	1.5	8.0	9.4	10.0	13.0 ± 0.7	12.5 ± 0.8 <sup>e</sup>
29,985.46	4f5d( <sup>3</sup> P <sup>o</sup> )6s <sup>4</sup> P <sup>o</sup>	0.5	9.9	11.7	12.3	15.7 ± 0.8	
30,417.46	4f5d( <sup>3</sup> P <sup>o</sup> )6s <sup>4</sup> P <sup>o</sup>	1.5	9.3	10.9	11.6	13.7 ± 0.7	13.6 ± 0.9 <sup>e</sup>
30,650.28	[4f5d( <sup>3</sup> G <sup>o</sup> )6s <sup>2</sup> G <sup>o</sup> ]	4.5	13.2	15.3	15.7	21.5 ± 1.1	20.8 ± 1.5 <sup>e</sup>
30,788.45	[4f5d( <sup>1</sup> F <sup>o</sup> )6s <sup>2</sup> F <sup>o</sup> ]	2.5	9.4	10.9	11.4		14.4 ± 1.2 <sup>f</sup>
30,896.84	4f5d( <sup>3</sup> P <sup>o</sup> )6s <sup>4</sup> P <sup>o</sup>	2.5	8.8	10.4	10.9	13.0 ± 0.7	18.6 ± 1.7 <sup>f</sup>
30,964.71	[4f5d( <sup>1</sup> F <sup>o</sup> )6s <sup>2</sup> F <sup>o</sup> ]	3.5	8.2	9.5	9.9	10.1 ± 0.5	11.9 ± 0.6 <sup>f</sup>
31,477.22	[5d <sup>2</sup> ( <sup>1</sup> G)6p <sup>2</sup> F <sup>o</sup> ]	2.5	5.9	6.7	7.0		8.7 ± 0.4 <sup>g</sup>
31,751.48	[4f5d( <sup>3</sup> D <sup>o</sup> )6s <sup>2</sup> D <sup>o</sup> ]	1.5	11.1	12.9	13.3		12.3 ± 0.8 <sup>g</sup>
32,140.55	[5d <sup>2</sup> ( <sup>1</sup> D)6p <sup>2</sup> F <sup>o</sup> ]	3.5	5.2	5.9	6.2	7.6 ± 0.4	7.3 ± 0.5 <sup>e</sup>

<sup>a</sup> Experimental energy levels and their LS-coupling designations taken from the NIST compilation [6]. Designations between brackets are tentative identifications deduced from the present HFR calculations; <sup>b</sup> This work (see text); <sup>c</sup> Experimental radiative lifetimes from Den Hartog et al. [22]; <sup>d</sup> Experimental radiative lifetimes from Biémont et al. [14]; <sup>e</sup> Experimental radiative lifetimes from Feng et al. [18]; <sup>f</sup> Experimental radiative lifetimes from Yarlagadda et al. [20]; <sup>g</sup> Experimental radiative lifetimes from Shang et al. [21].

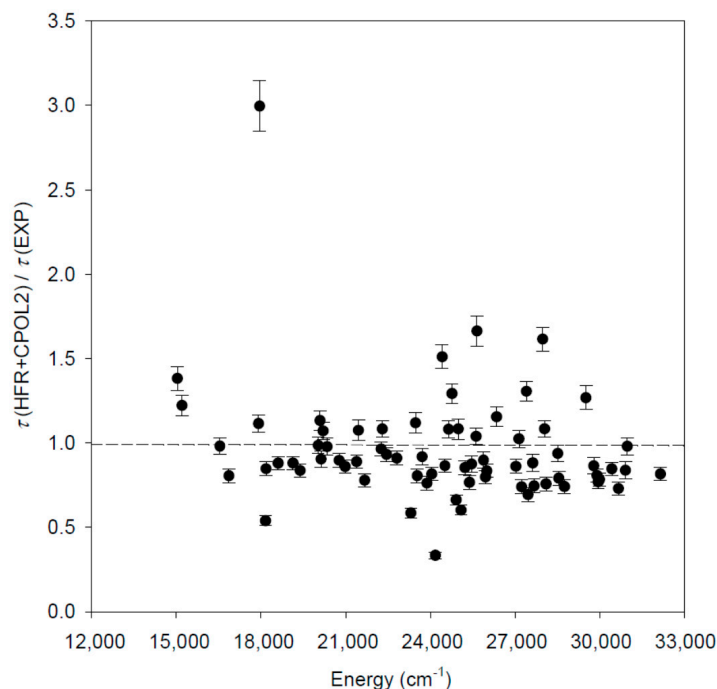


**Figure 2.** Comparison between the radiative lifetimes ( $\delta$ ) computed in the present work using the HFR+CPOL2 model and the most recent laser-induced fluorescence experimental measurements [22]. The dashed line indicates unity.

### 3.2. Oscillator Strengths and Transition Probabilities

In Table 2, we give the oscillator strengths and transition probabilities computed in the present work using the HFR+CPOL2 model, and rescaled using the experimental wavelengths, for a set of 392 La I transitions with  $\log gf$ -values greater than  $-1.0$ . These lines appear from the near-ultraviolet to the mid-infrared spectral regions, more precisely from 317 to 7843 nm. The experimental data recently published by Den Hartog et al. [22] are also reported for comparison in the table. There are 165 common transitions between this latter work and ours. For about three-quarter of these transitions, we note an agreement better than a factor of two between our calculated oscillator strengths and the experimental values while, for somewhat more than a half of the lines, the discrepancies between both sets of results do not exceed 25%. This is illustrated in Figure 3 where the HFR+CPOL2 and experimental  $\log gf$ -values are compared. It appears also that the calculated transition rates obtained in the present work can be considered as much more reliable than the theoretical data reported by Karaçoban and Özdemir [16] and Kurucz [8], these latter data being found to disagree by more than a factor of 2 with the experimental oscillator strengths, as highlighted in Figures 2 and 3 of [22].

Another interesting comparison is the one between the results obtained with the HFR+CPOL2 model and those deduced from our MCDHF computations, as described in Section 2.2. Such a comparison is shown in Figure 4. In this case, the agreement between both sets of oscillator strengths is found to be good in view of the complexity of the La I atomic structure, the discrepancies not exceeding 30% for half of the transitions (within the limit  $\log gf > -1$ ) and being anyway not larger than a factor of two for 95% of the entire set of common lines. A comparable agreement is observed when comparing our MCDHF calculations to the experimental  $gf$ -values of Den Hartog et al. [22], as illustrated in Figure 5. It is however to be emphasized that, on average, the MCDHF oscillator strengths tend to be slightly larger ( $\sim 10$ – $15\%$ ) than the HFR+CPOL2 and the experimental data, for the same reason as the one discussed in Section 3.1.

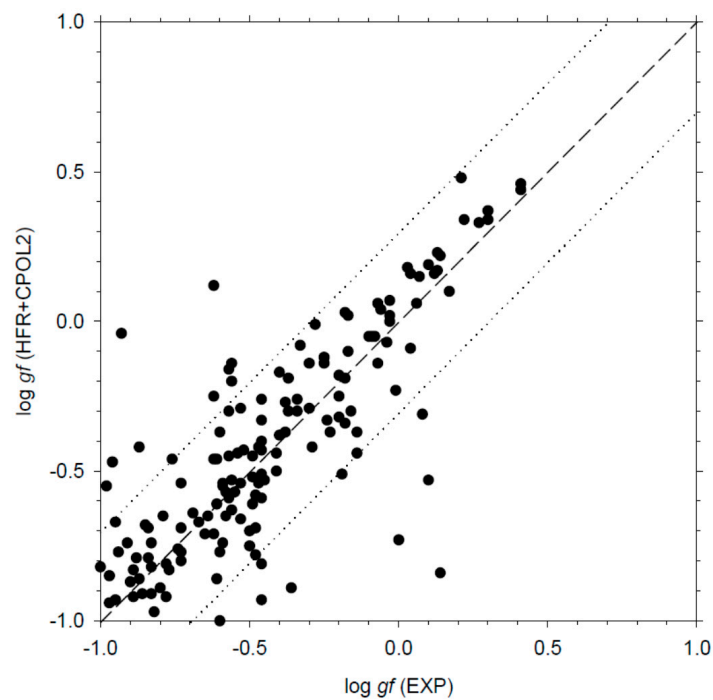


**Figure 3.** Comparison between the oscillator strengths ( $\log gf$ ) computed in the present work using the HFR+CPOL2 model and the available experimental values [22]. The dashed line corresponds to a perfect agreement while the dotted lines correspond to a discrepancy of a factor of two on the  $gf$ -values.

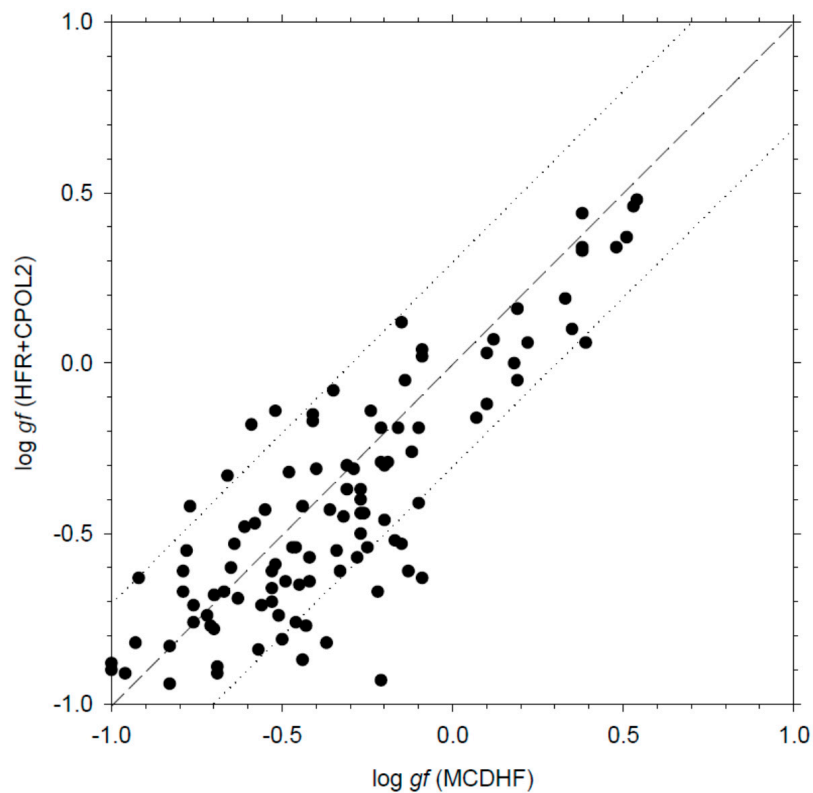


**Figure 4.** Comparison between the oscillator strengths ( $\log gf$ ) computed in the present work using the HFR+CPOL2 and the MCDHF models. The dashed line corresponds to a perfect agreement while the dotted lines correspond to a discrepancy of a factor of two on the  $gf$ -values.

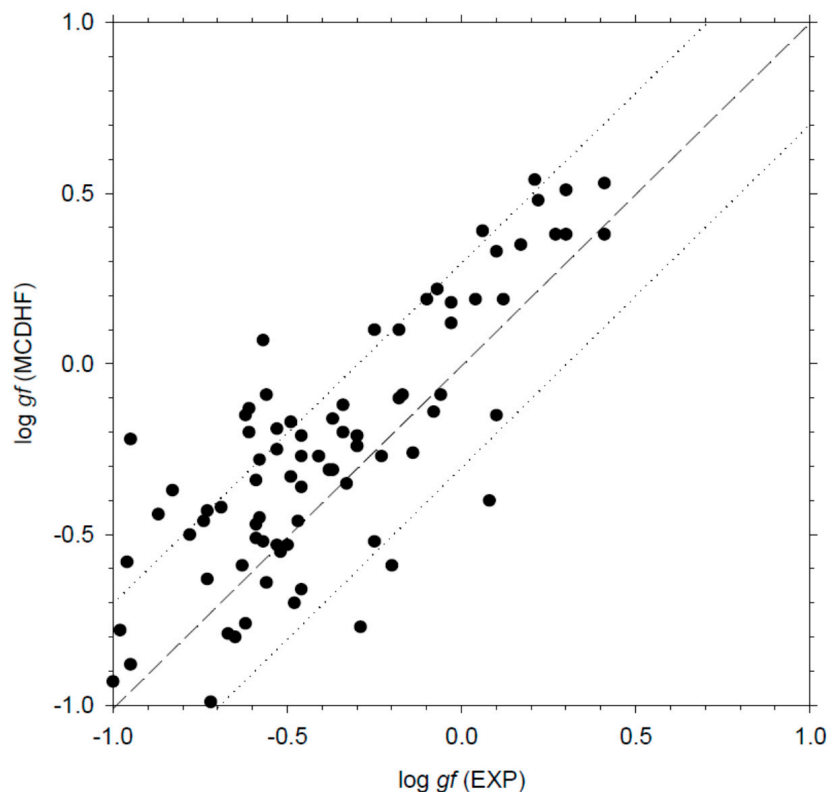


**Figure 5.** Comparison between the oscillator strengths ( $\log gf$ ) computed in the present work using the MCDHF model and the available experimental values [22]. The dashed line corresponds to a perfect agreement while the dotted lines correspond to a discrepancy of a factor of two on the  $gf$ -values.

A more robust method of evaluating uncertainties in  $gf$ - and  $gA$ -values for each calculated transition, as described by Kramida [34], is to plot the differences between theoretical and reference data (i.e., the experimental transition probabilities of Den Hartog et al. [22] in the present work) against the theoretical line strengths ( $S$ ). Such a plot is given in Figure 6 for the results reported in Table 2. From this figure, one can see that the entire range of calculated  $S$ -values can be divided into a few ranges, so that the average discrepancy is nearly constant in each range. Excluding a few outlying points shown in red in Figure 6, the root-mean-square deviations in the quantity  $\ln(gA_{\text{EXP}}/gA_{\text{HFR+CPOL2}})$  are 0.13, 0.28, 0.42, and 0.69 for  $S > 30$  a.u.,  $S = 15\text{--}30$  a.u.,  $S = 4.3\text{--}15$  a.u., and  $S < 4.3$  a.u., respectively. This corresponds to average relative deviations of 13%, 32%, 53%, and 98% for  $gA$  values. These estimates can be reliably extrapolated to calculated transitions for which there are no experimental data for comparison. Thus, a reliable estimate of uncertainty can be given for each calculated  $gA$  value of Table 2, even if there is no experimental data to compare with. From this evaluation, we found that among 227 transitions of Table 2 having no reference data, 8 calculated  $gA$ -values have an uncertainty of 13%, 19 have an uncertainty of 32%, 134 have an uncertainty of 53%, and only 66 are affected by larger uncertainties. This allowed us to give an evaluation of the uncertainty for each computed transition rate reported in Table 2, using the same code letter as the one usually employed in the NIST database [6]. The five abnormally deviating points shown in red in Figure 6 are probably due to insufficient accuracy of the calculated wavefunctions for the levels involved in the corresponding transitions. This was actually highlighted when comparing the calculated and experimental Landé  $g$ -factors for each upper odd level of these transitions, i.e., 23,303.26 ( $J = 7/2$ ), 24,409.68 ( $J = 7/2$ ), 24,639.26 ( $J = 3/2$ ), 25,083.36 ( $J = 7/2$ ), and 28,039.45 ( $J = 7/2$ )  $\text{cm}^{-1}$ , for which our  $g$ -values ( $g = 1.39, 1.34, 0.55, 1.22, \text{ and } 1.04$ ) showed rather large discrepancies with the experimental ones ( $g = 1.18, 1.16, 1.78, 1.38, \text{ and } 1.14$ ).

**Table 2.** Calculated oscillator strengths ( $\log gf$ ) and transition probabilities ( $gA$ ) for spectral lines in La I. A + B stands for  $A \times 10^B$ . Experimental data are also given where available, for comparison.

$\tilde{\nu}$ (nm) <sup>a</sup>	Lower Level <sup>b</sup>		Upper Level <sup>b</sup>		This Work <sup>c</sup>			Experiment <sup>d</sup>	
	$E$ (cm <sup>-1</sup> )	$J$	$E$ (cm <sup>-1</sup> )	$J$	$\log gf$	$gA$ (s <sup>-1</sup> )	Code	$\log gf$	$gA$ (s <sup>-1</sup> )
317.5982	0.000	1.5	31,477.22	2.5°	-0.74	1.20 + 08	E		
321.5810	1053.164	2.5	32,140.55	3.5°	-0.45	2.27 + 08	E	-0.49	2.08 + 08
324.7034	0.000	1.5	30,788.45	2.5°	-0.99	6.54 + 07	E		
334.2230	1053.164	2.5	30,964.71	3.5°	-0.37	2.55 + 08	E	-0.14	4.32 + 08
336.2042	1053.164	2.5	30,788.45	2.5°	-0.88	7.74 + 07	E		
340.4519	1053.164	2.5	30,417.46	1.5°	-0.94	6.60 + 07	E	-1.01	5.60 + 07
342.3726	0.000	1.5	29,199.57	1.5°	-0.73	1.05 + 08	E		
346.1184	1053.164	2.5	29,936.74	1.5°	-0.68	1.16 + 08	E	-0.85	7.84 + 07
348.0605	1053.164	2.5	29,775.58	2.5°	-0.96	6.01 + 07	E		
350.6980	0.000	1.5	28,506.41	2.5°	-0.87	7.23 + 07	E		
357.4425	0.000	1.5	27,968.54	1.5°	-0.44	1.89 + 08	E	-0.14	3.80 + 08
361.3074	0.000	1.5	27,669.37	2.5°	-0.54	1.47 + 08	E	-0.73	9.42 + 07
363.6661	1053.164	2.5	28,543.08	3.5°	-0.77	8.58 + 07	E	-0.94	5.76 + 07
364.1519	1053.164	2.5	28,506.41	2.5°	-0.10	4.03 + 08	D	0.04	5.46 + 08
370.4532	1053.164	2.5	28,039.45	3.5°	-0.80	7.65 + 07	E	-0.46	1.66 + 08
378.6495	1053.164	2.5	27,455.31	3.5°	-0.70	9.34 + 07	E		
385.2424	0.000	1.5	25,950.32	1.5°	-0.92	5.44 + 07	E	-1.57	1.20 + 07
387.8879	4121.572	4.5	29,894.91	3.5°	-0.91	5.47 + 07	E	-0.83	6.56 + 07
392.7551	0.000	1.5	25,453.95	0.5°	-0.30	2.14 + 08	D	-0.37	1.86 + 08
399.4164	3010.002	2.5	28,039.45	3.5°	-0.36	1.84 + 08	E	-1.19	2.72 + 07
401.5388	1053.164	2.5	25,950.32	1.5°	-0.18	2.71 + 08	D	-0.20	2.60 + 08
404.3371	2668.188	1.5	27,393.04	2.5°	-0.40	1.60 + 08	D		
406.0316	4121.572	4.5	28,743.24	5.5°	0.34	8.76 + 08	D+	0.22	6.72 + 08
406.4778	3494.526	3.5	28,089.17	4.5°	0.18	6.09 + 08	D+	0.03	4.32 + 08
407.9170	0.000	1.5	24,507.87	2.5°	-0.63	9.31 + 07	E	-0.56	1.11 + 08
408.9610	3010.002	2.5	27,455.31	3.5°	-0.14	2.91 + 08	D	-0.07	3.36 + 08
410.4870	2668.188	1.5	27,022.62	2.5°	-0.32	1.90 + 08	D	-0.20	2.47 + 08
410.9481	1053.164	2.5	25,380.27	3.5°	-0.68	8.21 + 07	E	-1.11	3.04 + 07
413.5538	0.000	1.5	24,173.83	1.5°	-0.60	9.77 + 07	E		
413.7031	1053.164	2.5	25,218.27	2.5°	-0.53	1.15 + 08	E	-0.53	1.15 + 08
414.3907	3494.526	3.5	27,619.54	4.5°	-0.83	5.70 + 07	E	-0.77	6.60 + 07
416.0258	1053.164	2.5	25,083.36	3.5°	0.12	5.10 + 08	E	-0.62	9.20 + 07
416.3303	3010.002	2.5	27,022.62	2.5°	-0.94	4.43 + 07	E	-0.97	4.08 + 07
417.1124	4121.572	4.5	28,089.17	4.5°	-0.82	5.81 + 07	E	-1.00	3.79 + 07
417.2310	3494.526	3.5	27,455.31	3.5°	-0.79	6.26 + 07	E	-0.84	5.52 + 07
417.7481	1053.164	2.5	24,984.29	2.5°	-0.70	7.69 + 07	E	-0.73	7.08 + 07
418.7310	0.000	1.5	23,874.95	2.5°	0.03	4.12 + 08	D	-0.06	3.31 + 08
421.6542	1053.164	2.5	24,762.60	1.5°	-0.93	4.37 + 07	E	-1.47	1.28 + 07
427.1148	7490.521	1.5	30,896.84	2.5°	-0.53	1.07 + 08	E	-0.45	1.30 + 08
428.0256	1053.164	2.5	24,409.68	3.5°	-0.53	1.07 + 08	E	0.10	4.55 + 08
429.3445	7679.939	2.5	30,964.71	3.5°	-0.79	5.90 + 07	E	-1.41	1.44 + 07
430.5996	7679.939	2.5	30,896.84	2.5°	-0.27	1.91 + 08	D	-0.38	1.51 + 08
431.1725	7231.407	0.5	30,417.46	1.5°	-0.74	6.50 + 07	E	-0.91	4.40 + 07
434.0720	8446.044	1.5	31,477.22	2.5°	-0.03	3.29 + 08	D		
435.4793	9183.797	2.5	32,140.55	3.5°	0.23	5.95 + 08	D+	0.13	4.72 + 08
440.2640	9044.214	0.5	31,751.48	1.5°	-0.39	1.39 + 08	D		
440.3015	7231.407	0.5	29,936.74	1.5°	-0.87	4.64 + 07	E	-0.90	4.36 + 07
442.3905	8052.162	3.5	30,650.28	4.5°	0.22	5.63 + 08	D+	0.14	4.65 + 08
444.2675	3494.526	3.5	25,997.17	4.5°	-0.93	3.95 + 07	E	-0.95	3.76 + 07
444.4197	7490.521	1.5	29,985.46	0.5°	-0.43	1.26 + 08	D	-0.52	1.00 + 08
445.2149	7011.909	2.5	29,466.67	3.5°	0.02	3.53 + 08	D+		
446.8965	3010.002	2.5	25,380.27	3.5°	-0.92	3.97 + 07	E	-0.89	4.24 + 07
447.4538	8446.044	1.5	30,788.45	2.5°	-0.38	1.39 + 08	D		
448.6053	7490.521	1.5	29,775.58	2.5°	-0.17	2.21 + 08	E	-0.40	1.31 + 08
449.1748	7679.939	2.5	29,936.74	1.5°	-0.44	1.20 + 08	D	-0.54	9.44 + 07
449.9040	9919.821	4.5	32,140.55	3.5°	-0.01	3.21 + 08	E	-0.28	1.71 + 08
450.0206	7679.939	2.5	29,894.91	3.5°	0.15	4.62 + 08	D+	0.07	3.83 + 08
450.1565	3010.002	2.5	25,218.27	2.5°	-0.66	7.16 + 07	E	-1.21	2.04 + 07
454.1773	7490.521	1.5	29,502.18	2.5°	-0.58	8.43 + 07	E	-0.46	1.12 + 08
454.9498	3010.002	2.5	24,984.29	2.5°	-0.94	3.73 + 07	E	-0.46	1.11 + 08
455.0164	2668.188	1.5	24,639.26	1.5°	-0.40	1.29 + 08	E	-1.57	8.68 + 06
455.0766	7231.407	0.5	29,199.57	1.5°	-0.65	7.28 + 07	E		
456.7904	3494.526	3.5	25,380.27	3.5°	-0.05	2.84 + 08	D	-0.09	2.62 + 08
457.0023	4121.572	4.5	25,997.17	4.5°	0.16	4.65 + 08	D+	0.13	4.34 + 08
458.1197	7679.939	2.5	29,502.18	2.5°	-0.19	2.03 + 08	E	-0.56	8.76 + 07
458.9890	9183.797	2.5	30,964.71	3.5°	-0.38	1.33 + 08	D		
459.8436	7231.407	0.5	28,971.84	1.5°	-0.80	4.99 + 07	E		
460.4237	9183.797	2.5	30,896.84	2.5°	-0.26	1.71 + 08	E	-0.46	1.08 + 08
461.5064	7231.407	0.5	28,893.51	0.5°	-0.49	1.01 + 08	D		

Table 2. Cont.

$\lambda$ (nm) <sup>a</sup>	Lower Level <sup>b</sup>		Upper Level <sup>b</sup>		This Work <sup>c</sup>			Experiment <sup>d</sup>	
	$E$ (cm <sup>-1</sup> )	$J$	$E$ (cm <sup>-1</sup> )	$J$	log $gf$	$gA$ (s <sup>-1</sup> )	Code	log $gf$	$gA$ (s <sup>-1</sup> )
462.2072	3010.002	2.5	24,639.26	1.5°	-0.97	3.38 + 07	E		
464.3129	7011.909	2.5	28,543.08	3.5°	-0.90	3.88 + 07	E	-1.01	3.05 + 07
464.6335	9960.904	3.5	31,477.22	2.5°	-0.03	2.85 + 08	D		
465.0322	3010.002	2.5	24,507.87	2.5°	-0.56	8.58 + 07	E	-0.98	3.24 + 07
465.1874	8446.044	1.5	29,936.74	1.5°	-0.86	4.26 + 07	E	-1.15	2.16 + 07
465.3905	7490.521	1.5	28,971.84	1.5°	-0.42	1.18 + 08	D		
470.2641	4121.572	4.5	25,380.27	3.5°	-0.83	4.44 + 07	E	-0.89	3.92 + 07
470.8186	9183.797	2.5	30,417.46	1.5°	-0.30	1.51 + 08	E	-0.57	8.12 + 07
473.3826	8446.044	1.5	29,564.70	0.5°	-0.66	6.44 + 07	E		
475.0419	9919.821	4.5	30,964.71	3.5°	-0.23	1.75 + 08	E	-0.01	2.88 + 08
475.9711	9960.904	3.5	30,964.71	3.5°	-0.97	3.16 + 07	E	-0.82	4.48 + 07
476.6891	0.000	1.5	20,972.17	2.5°	-0.46	1.02 + 08	D	-0.62	7.08 + 07
477.0425	7011.909	2.5	27,968.54	1.5°	-0.51	9.04 + 07	D	-0.46	1.02 + 08
479.9992	9960.904	3.5	30,788.45	2.5°	-0.33	1.35 + 08	D		
481.7112	8446.044	1.5	29,199.57	1.5°	-0.52	8.77 + 07	D		
481.7247	9183.797	2.5	29,936.74	1.5°	-0.86	3.96 + 07	E	-0.61	7.00 + 07
483.9514	7011.909	2.5	27,669.37	2.5°	0.02	3.01 + 08	D+	-0.03	2.63 + 08
485.0812	1053.164	2.5	21,662.51	3.5°	-0.46	9.76 + 07	E	-0.76	4.96 + 07
485.4950	9183.797	2.5	29,775.58	2.5°	-0.34	1.30 + 08	D	-0.24	1.62 + 08
487.0558	8446.044	1.5	28,971.84	1.5°	-0.73	5.21 + 07	E		
487.8848	8052.162	3.5	28,543.08	3.5°	-0.10	2.21 + 08	D	-0.17	1.90 + 08
488.7595	8052.162	3.5	28,506.41	2.5°	-0.15	1.97 + 08	E	-0.56	7.68 + 07
490.1867	1053.164	2.5	21,447.86	3.5°	-0.87	3.77 + 07	E	-0.87	3.76 + 07
492.0278	9183.797	2.5	29,502.18	2.5°	-0.75	4.93 + 07	E		
494.5845	7011.909	2.5	27,225.26	1.5°	-0.79	4.44 + 07	E	-0.88	3.64 + 07
494.9765	0.000	1.5	20,197.34	0.5°	-0.19	1.78 + 08	D	-0.18	1.80 + 08
497.7952	0.000	1.5	20,082.98	1.5°	-0.94	3.07 + 07	E	-1.35	1.20 + 07
500.1785	8052.162	3.5	28,039.45	3.5°	-0.50	8.39 + 07	E	-0.19	1.70 + 08
504.6871	3494.526	3.5	23,303.26	3.5°	-0.40	1.04 + 08	D	-0.46	9.04 + 07
505.0564	3010.002	2.5	22,804.25	2.5°	-0.29	1.34 + 08	D	-0.30	1.30 + 08
505.6459	2668.188	1.5	22,439.36	1.5°	-0.43	9.74 + 07	D	-0.46	9.04 + 07
510.6233	2668.188	1.5	22,246.64	0.5°	-0.05	2.30 + 08	D+	-0.08	2.10 + 08
511.4489	9919.821	4.5	29,466.67	3.5°	-0.76	4.47 + 07	E		
514.5417	3010.002	2.5	22,439.36	1.5°	0.16	3.67 + 08	D+	0.12	3.28 + 08
515.2367	8052.162	3.5	27,455.31	3.5°	-0.77	4.28 + 07	E		
515.8681	0.000	1.5	19,379.40	2.5°	-0.57	6.75 + 07	D	-0.58	6.60 + 07
516.7783	4121.572	4.5	23,466.84	4.5°	-0.80	3.94 + 07	E	-0.73	4.60 + 07
517.7296	3494.526	3.5	22,804.25	2.5°	0.34	5.46 + 08	C+	0.30	4.92 + 08
517.9119	8446.044	1.5	27,748.97	0.5°	-0.76	4.36 + 07	E		
518.3910	1053.164	2.5	20,338.25	2.5°	-0.90	3.09 + 07	E	-0.86	3.42 + 07
521.1854	4121.572	4.5	23,303.26	3.5°	0.48	7.40 + 08	E	0.21	3.98 + 08
523.4274	4121.572	4.5	23,221.10	3.5°	-0.84	3.52 + 07	E	0.14	3.38 + 08
527.1174	1053.164	2.5	20,018.99	1.5°	0.03	2.56 + 08	E	-0.18	1.60 + 08
527.6413	8446.044	1.5	27,393.04	2.5°	-0.58	6.36 + 07	D	-0.48	7.98 + 07
530.1974	9183.797	2.5	28,039.45	3.5°	-0.43	8.75 + 07	D		
530.4012	7490.521	1.5	26,338.93	2.5°	-0.68	4.90 + 07	E	-0.48	7.80 + 07
532.3555	8446.044	1.5	27,225.26	1.5°	-0.67	5.03 + 07	E	-0.95	2.64 + 07
534.0705	7231.407	0.5	25,950.32	1.5°	-0.96	2.57 + 07	E		
535.7856	7679.939	2.5	26,338.93	2.5°	-0.25	1.32 + 08	D	-0.20	1.48 + 08
536.8136	9919.821	4.5	28,543.08	3.5°	-0.61	5.67 + 07	D		
538.0005	9960.904	3.5	28,543.08	3.5°	-0.71	4.45 + 07	E	-0.65	5.20 + 07
545.5142	1053.164	2.5	19,379.40	2.5°	0.16	3.23 + 08	D+	0.04	2.44 + 08
547.5155	9919.821	4.5	28,179.07	5.5°	-0.32	1.07 + 08	D		
549.1060	7011.909	2.5	25,218.27	2.5°	-0.68	4.61 + 07	E	-0.84	3.24 + 07
550.1337	0.000	1.5	18,172.35	1.5°	0.07	2.61 + 08	D+	-0.03	2.05 + 08
550.2246	9919.821	4.5	28,089.17	4.5°	-0.77	3.74 + 07	E	-0.60	5.60 + 07
551.5274	7490.521	1.5	25,616.95	0.5°	-0.45	7.79 + 07	D	-0.61	5.32 + 07
551.7344	9919.821	4.5	28,039.45	3.5°	-0.72	4.18 + 07	E	0.00	2.21 + 08
552.9882	9960.904	3.5	28,039.45	3.5°	-0.24	1.25 + 08	E	-0.62	5.20 + 07
554.1249	9183.797	2.5	27,225.26	1.5°	-0.14	1.57 + 08	D	-0.25	1.22 + 08
554.4916	9719.439	1.5	27,748.97	0.5°	-0.43	8.07 + 07	D		
556.5434	7679.939	2.5	25,643.00	1.5°	-0.32	1.02 + 08	D	-0.46	7.44 + 07
556.9905	9183.797	2.5	27,132.44	3.5°	-0.49	6.91 + 07	D		
558.5518	7011.909	2.5	24,910.38	1.5°	-0.94	2.46 + 07	E		
558.8328	3494.526	3.5	21,384.00	4.5°	-0.61	5.27 + 07	D	-0.49	6.90 + 07
563.1222	3010.002	2.5	20,763.21	3.5°	-0.50	6.71 + 07	D	-0.41	8.16 + 07
564.5449	9960.904	3.5	27,669.37	2.5°	-0.71	4.09 + 07	E		
564.8239	9919.821	4.5	27,619.54	4.5°	0.44	5.73 + 08	C+	0.41	5.33 + 08
565.4868	7231.407	0.5	24,910.38	1.5°	-0.48	6.90 + 07	E	-0.96	2.28 + 07
565.6586	9719.439	1.5	27,393.04	2.5°	-0.64	4.73 + 07	E	-0.64	4.80 + 07
565.7719	2668.188	1.5	20,338.25	2.5°	-0.64	4.72 + 07	E	-0.58	5.52 + 07

Table 2. Cont.

$\lambda$ (nm) <sup>a</sup>	Lower Level <sup>b</sup>		Upper Level <sup>b</sup>		This Work <sup>c</sup>			Experiment <sup>d</sup>	
	$E$ (cm <sup>-1</sup> )	$J$	$E$ (cm <sup>-1</sup> )	$J$	log $gf$	$gA$ (s <sup>-1</sup> )	Code	log $gf$	$gA$ (s <sup>-1</sup> )
567.1428	7011.909	2.5	24,639.26	1.5°	-0.89	2.70 + 07	E		
570.2536	7231.407	0.5	24,762.60	1.5°	-0.84	2.95 + 07	E		
571.4527	9960.904	3.5	27,455.31	3.5°	-0.55	5.79 + 07	D		
571.4735	7490.521	1.5	24,984.29	2.5°	-0.78	3.41 + 07	E		
573.4941	9960.904	3.5	27,393.04	2.5°	-0.88	2.64 + 07	E	-0.36	8.94 + 07
574.0652	2668.188	1.5	20,082.98	1.5°	-0.07	1.71 + 08	E	-0.33	9.52 + 07
574.4403	7679.939	2.5	25,083.36	3.5°	-0.31	9.91 + 07	E	0.08	2.44 + 08
576.9324	3010.002	2.5	20,338.25	2.5°	0.01	2.03 + 08	D+	-0.03	1.87 + 08
577.7682	9719.439	1.5	27,022.62	2.5°	-0.96	2.22 + 07	E		
578.8086	7490.521	1.5	24,762.60	1.5°	-0.33	9.40 + 07	D		
578.9224	3494.526	3.5	20,763.21	3.5°	0.19	3.09 + 08	D+	0.10	2.48 + 08
579.1322	4121.572	4.5	21,384.00	4.5°	0.37	4.65 + 08	C	0.30	3.93 + 08
580.8081	9919.821	4.5	27,132.44	3.5°	-0.40	7.82 + 07	D		
582.1977	9960.904	3.5	27,132.44	3.5°	0.10	2.46 + 08	D+	0.17	2.94 + 08
582.3818	8052.162	3.5	25,218.27	2.5°	-0.37	8.40 + 07	D	-0.40	7.86 + 07
582.5238	7011.909	2.5	24,173.83	1.5°	-0.48	6.52 + 07	D		
582.7543	9183.797	2.5	26,338.93	2.5°	-0.37	8.47 + 07	E	-0.60	4.92 + 07
584.8365	9960.904	3.5	27,054.96	4.5°	-0.17	1.33 + 08	D		
585.2267	7679.939	2.5	24,762.60	1.5°	-0.43	7.29 + 07	E	-0.87	2.64 + 07
585.5586	3010.002	2.5	20,082.98	1.5°	-0.80	3.07 + 07	E	-0.78	3.24 + 07
586.9950	8052.162	3.5	25,083.36	3.5°	-0.89	2.51 + 07	E	-1.16	1.33 + 07
587.4728	7490.521	1.5	24,507.87	2.5°	-0.53	5.77 + 07	D	-0.49	6.18 + 07
590.4296	8052.162	3.5	24,984.29	2.5°	-0.89	2.49 + 07	E	-1.01	1.86 + 07
593.0608	1053.164	2.5	17,910.17	3.5°	-0.57	5.08 + 07	D	-0.55	5.36 + 07
593.0681	0.000	1.5	16,856.80	2.5°	-0.66	4.14 + 07	E	-0.79	3.10 + 07
593.5285	3494.526	3.5	20,338.25	2.5°	-0.76	3.26 + 07	E	-0.73	3.54 + 07
596.0586	8446.044	1.5	25,218.27	2.5°	-0.73	3.48 + 07	E	-0.83	2.76 + 07
597.5723	7679.939	2.5	24,409.68	3.5°	-0.04	1.70 + 08	E	-0.93	2.19 + 07
599.5495	13,631.04	2.5°	30,305.61	2.5	-0.73	3.43 + 07	E		
600.7360	4121.572	4.5	20,763.21	3.5°	-0.82	2.82 + 07	E	-0.83	2.80 + 07
601.7140	13,260.38	1.5°	29,874.97	1.5	-0.35	8.22 + 07	D		
603.8588	7490.521	1.5	24,046.10	2.5°	-0.29	9.47 + 07	E	-0.53	5.40 + 07
606.8711	7231.407	0.5	23,704.81	1.5°	-0.54	5.27 + 07	D	-0.59	4.68 + 07
607.0418	15,219.89	0.5°	31,688.66	1.5	-0.99	1.86 + 07	E		
607.5237	8052.162	3.5	24,507.87	2.5°	-0.91	2.23 + 07	E		
610.8477	7679.939	2.5	24,046.10	2.5°	-0.30	9.01 + 07	D	-0.34	8.16 + 07
612.1221	15,019.51	3.5°	31,351.60	2.5	-0.65	4.00 + 07	D		
612.5770	15,031.64	1.5°	31,351.60	2.5	-0.93	2.09 + 07	E		
613.4384	7231.407	0.5	23,528.45	0.5°	-0.54	5.08 + 07	D	-0.59	4.60 + 07
614.2961	13,631.04	2.5°	29,905.33	2.5	-0.13	1.32 + 08	D+		
614.5306	15,019.51	3.5°	31,287.59	3.5	-0.61	4.32 + 07	D		
616.4989	15,031.64	1.5°	31,247.78	1.5	-0.42	6.66 + 07	D		
616.5693	7490.521	1.5	23,704.81	1.5°	-0.43	6.46 + 07	D	-0.41	6.80 + 07
621.8210	9919.821	4.5	25,997.17	4.5°	-0.95	1.95 + 07	E		
621.9456	14,095.69	0.5°	30,169.82	1.5	-0.62	4.12 + 07	D		
623.4838	9183.797	2.5	25,218.27	2.5°	-0.80	2.72 + 07	E		
624.9909	4121.572	4.5	20,117.38	5.5°	0.46	4.95 + 08	C+	0.41	4.42 + 08
626.6013	9919.821	4.5	25,874.52	5.5°	0.06	1.94 + 08	D+	0.06	1.94 + 08
627.8270	14,095.69	0.5°	30,019.24	0.5	-0.84	2.46 + 07	E		
629.3556	3494.526	3.5	19,379.40	2.5°	-0.92	2.03 + 07	E	-0.78	2.76 + 07
630.8216	15,503.64	2.5°	31,351.60	2.5	-0.19	1.07 + 08	D		
631.7500	16,099.29	3.5°	31,923.96	4.5	-0.52	5.02 + 07	D		
632.5908	1053.164	2.5	16,856.80	2.5°	-0.90	2.09 + 07	E	-0.80	2.62 + 07
633.3798	15,503.64	2.5°	31,287.59	3.5	-0.59	4.28 + 07	D		
635.6416	8446.044	1.5	24,173.83	1.5°	-0.45	5.82 + 07	D		
637.5467	16,243.17	4.5°	31,923.96	4.5	-0.85	2.32 + 07	E		
639.4227	3494.526	3.5	19,129.31	4.5°	0.33	3.45 + 08	C+	0.27	3.01 + 08
640.9845	14,708.92	1.5°	30,305.61	2.5	-0.83	2.41 + 07	E		
641.0984	3010.002	2.5	18,603.92	3.5°	0.06	1.85 + 08	D+	-0.07	1.37 + 08
642.6591	15,503.64	2.5°	31,059.69	3.5	-0.99	1.67 + 07	E		
645.0317	9719.439	1.5	25,218.27	2.5°	-0.69	3.27 + 07	D		
645.4502	2668.188	1.5	18,156.97	2.5°	-0.17	1.09 + 08	E	-0.57	4.32 + 07
645.5984	1053.164	2.5	16,538.39	3.5°	-0.26	8.74 + 07	D	-0.34	7.36 + 07
648.5531	8052.162	3.5	23,466.84	4.5°	-0.64	3.61 + 07	D	-0.69	3.30 + 07
650.6187	14,804.08	2.5°	30,169.82	1.5	-0.38	6.60 + 07	D		
652.3878	9183.797	2.5	24,507.87	2.5°	-0.85	2.24 + 07	E		
652.9738	14,708.92	1.5°	30,019.24	0.5	-0.29	8.10 + 07	D		
654.0084	15,019.51	3.5°	30,305.61	2.5	-0.23	9.16 + 07	D		
656.5950	9183.797	2.5	24,409.68	3.5°	-0.87	2.06 + 07	E		
657.8502	0.000	1.5	15,196.83	2.5°	-0.61	3.81 + 07	D	-0.61	3.84 + 07
658.2197	16,099.29	3.5°	31,287.59	3.5	0.08	1.84 + 08	D+		

Table 2. Cont.

$\lambda$ (nm) <sup>a</sup>	Lower Level <sup>b</sup>		Upper Level <sup>b</sup>		This Work <sup>c</sup>			Experiment <sup>d</sup>	
	$E$ (cm <sup>-1</sup> )	$J$	$E$ (cm <sup>-1</sup> )	$J$	log $gf$	$gA$ (s <sup>-1</sup> )	Code	log $gf$	$gA$ (s <sup>-1</sup> )
660.0158	3010.002	2.5	18,156.97	2.5°	-0.93	1.82 + 07	E	-1.02	1.47 + 07
660.7728	9044.214	0.5	24,173.83	1.5°	-0.68	3.16 + 07	D		
660.8239	9960.904	3.5	25,089.35	4.5°	-0.16	1.06 + 08	D+		
661.6572	3494.526	3.5	18,603.92	3.5°	-0.76	2.62 + 07	E	-0.74	2.78 + 07
663.3476	14,804.08	2.5°	29,874.97	1.5	-0.47	5.17 + 07	D		
664.5148	16,243.17	4.5°	31,287.59	3.5	0.18	2.30 + 08	C+		
666.1390	4121.572	4.5	19,129.31	4.5°	-0.74	2.71 + 07	E	-0.59	3.90 + 07
667.6849	15,196.83	2.5°	30,169.82	1.5	-0.80	2.39 + 07	E		
670.9481	3010.002	2.5	17,910.17	3.5°	-0.37	6.26 + 07	D	-0.23	8.72 + 07
671.5948	15,019.51	3.5°	29,905.33	2.5	-0.67	3.18 + 07	D		
674.8109	8446.044	1.5	23,260.92	0.5°	-0.84	2.12 + 07	E		
682.3775	7011.909	2.5	21,662.51	3.5°	-0.78	2.36 + 07	E	-0.48	4.72 + 07
691.6659	17,023.36	3.5	31,477.22	2.5°	-0.98	1.45 + 07	E		
692.5240	7011.909	2.5	21,447.86	3.5°	-0.14	9.96 + 07	D+	-0.30	6.96 + 07
697.6842	9919.821	4.5	24,249.00	4.5°	-0.62	3.25 + 07	D		
702.3688	8052.162	3.5	22,285.77	4.5°	-0.06	1.18 + 08	D+	-0.10	1.07 + 08
703.2039	9044.214	0.5	23,260.92	0.5°	-0.62	3.24 + 07	D		
704.5963	2668.188	1.5	16,856.80	2.5°	-0.43	4.97 + 07	D	-0.47	4.50 + 07
705.9527	17,947.13	2.5°	32,108.48	3.5	-0.74	2.41 + 07	E		
707.6374	9960.904	3.5	24,088.54	3.5°	-0.71	2.61 + 07	D		
712.7473	15,019.51	3.5°	29,045.86	3.5	-0.82	1.99 + 07	E		
716.1216	7011.909	2.5	20,972.17	2.5°	-0.12	9.90 + 07	D+	-0.25	7.32 + 07
716.6031	14,804.08	2.5°	28,754.96	2.5	-0.97	1.39 + 07	E		
723.1903	17,140.90	4.5	30,964.71	3.5°	-0.60	3.18 + 07	D		
726.2753	17,023.36	3.5	30,788.45	2.5°	-0.25	7.17 + 07	D		
734.5327	8052.162	3.5	21,662.51	3.5°	0.02	1.29 + 08	E	-0.17	8.24 + 07
737.9665	9919.821	4.5	23,466.84	4.5°	-0.30	6.11 + 07	D	-0.16	8.60 + 07
738.2683	9719.439	1.5	23,260.92	0.5°	-0.58	3.22 + 07	D		
739.6431	18,172.35	1.5°	31,688.66	1.5	-0.35	5.39 + 07	D		
743.7636	17,910.17	3.5°	31,351.60	2.5	-0.67	2.59 + 07	D		
745.8144	17,947.13	2.5°	31,351.60	2.5	-0.95	1.35 + 07	E		
746.3028	8052.162	3.5	21,447.86	3.5°	-0.71	2.35 + 07	E	-0.50	3.76 + 07
749.3930	17,947.13	2.5°	31,287.59	3.5	-0.39	4.83 + 07	D		
750.9376	16,856.80	2.5°	30,169.82	1.5	-0.85	1.69 + 07	E		
756.8598	17,910.17	3.5°	31,119.02	2.5	-0.83	1.71 + 07	E		
763.6844	18,156.97	2.5°	31,247.78	1.5	-0.32	5.53 + 07	D		
767.9457	16,856.80	2.5°	29,874.97	1.5	-0.44	4.07 + 07	D		
781.2982	19,129.31	4.5°	31,925.00	3.5	-0.70	2.16 + 07	D		
784.2407	18,603.92	3.5°	31,351.60	2.5	-0.36	4.69 + 07	D		
790.3695	18,315.88	4.5	30,964.71	3.5°	-0.34	4.84 + 07	D		
796.1502	17,797.29	1.5°	30,354.28	2.5	-0.91	1.28 + 07	E		
796.8730	19,379.40	2.5°	31,925.00	3.5	-0.65	2.35 + 07	D		
798.8150	18,603.92	3.5°	31,119.02	2.5	-0.56	2.85 + 07	D		
800.1873	3010.002	2.5	15,503.64	2.5°	-0.95	1.16 + 07	E		
802.8791	17,567.49	0.5°	30,019.24	0.5	-1.00	1.04 + 07	E		
808.4499	9919.821	4.5	22,285.77	4.5°	-0.46	3.56 + 07	D	-0.57	2.70 + 07
810.1920	18,310.92	5.5	30,650.28	4.5°	-0.33	4.71 + 07	D		
811.0853	17,140.90	4.5	29,466.67	3.5°	-0.37	4.33 + 07	D		
816.1092	13,747.276	4.5	25,997.17	4.5°	-0.98	1.05 + 07	E		
824.7470	4121.572	4.5	16,243.17	4.5°	-0.75	1.76 + 07	D		
832.4721	3494.526	3.5	15,503.64	2.5°	-0.63	2.24 + 07	D		
833.4405	17,910.17	3.5°	29,905.33	2.5	-0.34	4.39 + 07	D		
834.6542	4121.572	4.5	16,099.29	3.5°	-0.30	4.83 + 07	D		
837.9660	19,129.31	4.5°	31,059.69	3.5	-0.09	7.73 + 07	D+		
846.7526	20,117.38	5.5°	31,923.96	4.5	0.12	1.24 + 08	C+		
851.3598	9919.821	4.5	21,662.51	3.5°	-0.76	1.61 + 07	D		
852.0643	18,172.35	1.5°	29,905.33	2.5	-0.78	1.54 + 07	D		
854.3427	18,603.92	3.5°	30,305.61	2.5	-0.99	9.33 + 06	E		
854.3488	9960.904	3.5	21,662.51	3.5°	-0.67	1.95 + 07	D	-0.53	2.72 + 07
854.5451	3010.002	2.5	14,708.92	1.5°	-0.75	1.62 + 07	D		
855.9080	19,379.40	2.5°	31,059.69	3.5	-0.66	1.97 + 07	D		
863.3930	18,315.88	4.5	29,894.91	3.5°	-0.66	1.96 + 07	D		
867.2120	9919.821	4.5	21,447.86	3.5°	-0.76	1.55 + 07	E	-0.50	2.80 + 07
867.4419	3494.526	3.5	15,019.51	3.5°	-0.95	9.87 + 06	E		
870.3136	9960.904	3.5	21,447.86	3.5°	-0.75	1.58 + 07	D		
874.8416	2668.188	1.5	14,095.69	0.5°	-0.92	1.04 + 07	E		
880.1268	20,392.60	0.5	31,751.48	1.5°	-0.73	1.60 + 07	D		
881.8966	13,747.276	4.5	25,083.36	3.5°	-0.97	9.24 + 06	E		
882.1670	20,018.99	1.5°	31,351.60	2.5	-0.70	1.72 + 07	D		
882.5854	8052.162	3.5	19,379.40	2.5°	-0.53	2.54 + 07	D	-0.56	2.34 + 07

Table 2. Cont.

$\lambda$ (nm) <sup>a</sup>	Lower Level <sup>b</sup>		Upper Level <sup>b</sup>		This Work <sup>c</sup>			Experiment <sup>d</sup>	
	$E$ (cm <sup>-1</sup> )	$J$	$E$ (cm <sup>-1</sup> )	$J$	log $gf$	$gA$ (s <sup>-1</sup> )	Code	log $gf$	$gA$ (s <sup>-1</sup> )
895.6565	18,037.64	1.5	29,199.57	1.5°	-0.86	1.16 + 07	E		
895.7760	7011.909	2.5	18,172.35	1.5°	-0.67	1.79 + 07	D	-0.67	1.80 + 07
904.6930	20,197.34	0.5°	31,247.78	1.5	-0.81	1.25 + 07	D		
907.9116	9960.904	3.5	20,972.17	2.5°	-0.42	3.05 + 07	D	-0.29	4.14 + 07
908.9274	18,776.62	2.5	29,775.58	2.5°	-0.82	1.23 + 07	D		
912.7555	20,972.17	2.5°	31,925.00	3.5	-0.98	8.30 + 06	E		
915.7172	12,787.404	2.5	23,704.81	1.5°	-0.78	1.33 + 07	D		
922.6653	9183.797	2.5	20,018.99	1.5°	-0.91	9.60 + 06	E		
925.0058	13,238.323	3.5	24,046.10	2.5°	-0.59	2.02 + 07	D	-0.57	2.10 + 07
932.8854	20,972.17	2.5°	31,688.66	1.5	-0.68	1.60 + 07	D		
937.6175	13,747.276	4.5	24,409.68	3.5°	-0.59	1.94 + 07	D		
948.5100	21,384.00	4.5°	31,923.96	4.5	0.05	8.38 + 07	C+		
954.1972	21,447.86	3.5°	31,925.00	3.5	-0.70	1.46 + 07	D		
957.0444	21,662.51	3.5°	32,108.48	3.5	-0.94	8.39 + 06	E		
964.0855	17,023.36	3.5	27,393.04	2.5°	-0.33	3.34 + 07	D	-0.18	4.74 + 07
970.9394	20,763.21	3.5°	31,059.69	3.5	-0.14	5.13 + 07	D+		
972.9114	20,972.17	2.5°	31,247.78	1.5	-0.85	1.00 + 07	D		
973.7092	7679.939	2.5	17,947.13	2.5°	-0.85	9.90 + 06	D	-0.97	7.50 + 06
974.1552	21,662.51	3.5°	31,925.00	3.5	-0.47	2.39 + 07	D		
977.5166	18,315.88	4.5	28,543.08	3.5°	-0.74	1.27 + 07	D		
980.4358	21,943.80	3.5	32,140.55	3.5°	-0.75	1.24 + 07	D		
985.2573	20,972.17	2.5°	31,119.02	2.5	-0.33	3.20 + 07	D+		
991.1190	20,082.98	1.5°	30,169.82	1.5	-0.59	1.76 + 07	D		
999.7999	17,023.36	3.5	27,022.62	2.5°	-0.86	9.30 + 06	D		
1000.5724	17,140.90	4.5	27,132.44	3.5°	-0.07	5.64 + 07	D+	-0.04	6.08 + 07
1002.9997	20,338.25	2.5°	30,305.61	2.5	-0.59	1.69 + 07	D		
1006.6821	18,037.64	1.5	27,968.54	1.5°	-0.98	6.93 + 06	E		
1011.2194	20,018.99	1.5°	29,905.33	2.5	-0.77	1.10 + 07	D		
1013.0834	18,310.92	5.5	28,179.07	5.5°	-0.85	9.24 + 06	D		
1017.7700	22,285.77	4.5°	32,108.48	3.5	-0.74	1.18 + 07	D		
1018.4625	12,430.609	1.5	22,246.64	0.5°	-0.70	1.28 + 07	D	-0.62	1.54 + 07
1020.9630	20,082.98	1.5°	29,874.97	1.5	-0.90	8.08 + 06	E		
1021.9890	21,969.32	2.5	31,751.48	1.5°	-0.34	2.90 + 07	D+		
1027.4898	18,776.62	2.5	28,506.41	2.5°	-0.48	2.08 + 07	D		
1028.1470	18,315.88	4.5	28,039.45	3.5°	-0.36	2.74 + 07	D		
1029.4429	18,037.64	1.5	27,748.97	0.5°	-0.98	6.59 + 06	E		
1031.8059	21,662.51	3.5°	31,351.60	2.5	-0.87	8.44 + 06	D		
1033.0277	20,197.34	0.5°	29,874.97	1.5	-0.85	8.77 + 06	D		
1033.2348	21,384.00	4.5°	31,059.69	3.5	-0.75	1.11 + 07	D		
1033.7188	21,447.86	3.5°	31,119.02	2.5	-0.33	2.95 + 07	D+		
1034.9172	9719.439	1.5	19,379.40	2.5°	-0.77	1.05 + 07	D		
1035.7755	12,787.404	2.5	22,439.36	1.5°	-0.54	1.81 + 07	D	-0.47	2.12 + 07
1037.1430	22,285.77	4.5°	31,925.00	3.5	-0.18	4.14 + 07	D+		
1044.9646	20,338.25	2.5°	29,905.33	2.5	-0.90	7.62 + 06	E		
1045.0906	13,238.323	3.5	22,804.25	2.5°	-0.37	2.61 + 07	D	-0.38	2.58 + 07
1046.1780	13,747.276	4.5	23,303.26	3.5°	-0.19	3.92 + 07	D	-0.37	2.64 + 07
1048.2913	20,338.25	2.5°	29,874.97	1.5	-0.94	6.99 + 06	E		
1048.6541	21,943.80	3.5	31,477.22	2.5°	-0.89	7.86 + 06	D		
1051.4688	21,969.32	2.5	31,477.22	2.5°	-0.98	6.37 + 06	E		
1057.1829	21,662.51	3.5°	31,119.02	2.5	-0.90	7.46 + 06	D		
1063.8575	21,662.51	3.5°	31,059.69	3.5	-0.94	6.84 + 06	E		
1073.9789	18,310.92	5.5	27,619.54	4.5°	0.10	7.22 + 07	C+		
1093.5386	20,763.21	3.5°	29,905.33	2.5	-0.82	8.48 + 06	D		
1093.8605	18,315.88	4.5	27,455.31	3.5°	-0.61	1.36 + 07	D		
1096.1008	22,804.25	2.5°	31,925.00	3.5	-0.85	7.80 + 06	D		
1110.6662	22,246.64	0.5°	31,247.78	1.5	-0.86	7.49 + 06	D		
1115.9028	16,991.42	0.5	25,950.32	1.5°	-0.92	6.41 + 06	D		
1121.7452	22,439.36	1.5°	31,351.60	2.5	-0.82	7.94 + 06	D		
1128.6458	21,447.86	3.5°	30,305.61	2.5	-0.87	7.02 + 06	D		
1139.4294	22,285.77	4.5°	31,059.69	3.5	-0.82	7.73 + 06	D		
1143.9720	18,315.88	4.5	27,054.96	4.5°	-0.78	8.40 + 06	D		
1144.6872	17,140.90	4.5	25,874.52	5.5°	-0.89	6.49 + 06	D		
1145.6378	9183.797	2.5	17,910.17	3.5°	-0.86	7.05 + 06	D		
1151.2147	9919.821	4.5	18,603.92	3.5°	-0.96	5.46 + 06	E		
1151.8035	22,439.36	1.5°	31,119.02	2.5	-0.67	1.07 + 07	D		
1154.5037	20,082.98	1.5°	28,742.34	1.5	-0.96	5.52 + 06	E		
1159.6811	23,303.26	3.5°	31,923.96	4.5	-0.09	4.07 + 07	C+		
1182.0631	21,447.86	3.5°	29,905.33	2.5	-0.69	9.73 + 06	D		
1183.2985	18,776.62	2.5	27,225.26	1.5°	-0.93	5.56 + 06	D		
1187.7876	20,338.25	2.5°	28,754.96	2.5	-0.87	6.41 + 06	D		
1202.3500	22,804.25	2.5°	31,119.02	2.5	-0.95	5.20 + 06	D		
1207.0127	20,763.21	3.5°	29,045.86	3.5	-0.88	5.98 + 06	D		

Table 2. Cont.

$\lambda$ (nm) <sup>a</sup>	Lower Level <sup>b</sup>		Upper Level <sup>b</sup>		This Work <sup>c</sup>			Experiment <sup>d</sup>	
	$E$ (cm <sup>-1</sup> )	$J$	$E$ (cm <sup>-1</sup> )	$J$	log $gf$	$gA$ (s <sup>-1</sup> )	Code	log $gf$	$gA$ (s <sup>-1</sup> )
1210.9910	22,804.25	2.5°	31,059.69	3.5	-0.39	1.87 + 07	D+		
1245.3833	16,735.14	1.5	24,762.60	1.5°	-0.84	6.21 + 06	D		
1251.1674	9919.821	4.5	17,910.17	3.5°	-0.69	8.60 + 06	D		
1252.1106	23,303.26	3.5°	31,287.59	3.5	-0.62	1.03 + 07	D		
1279.4518	23,874.95	2.5°	31,688.66	1.5	-0.47	1.39 + 07	D		
1293.2303	22,439.36	1.5°	30,169.82	1.5	-0.89	5.13 + 06	D		
1300.6688	18,310.92	5.5	25,997.17	4.5°	-0.96	4.32 + 06	D		
1304.5776	17,099.38	2.5	24,762.60	1.5°	-0.68	8.17 + 06	D		
1306.4272	12,430.609	1.5	20,082.98	1.5°	-0.65	8.66 + 06	D		
1309.1039	13,747.276	4.5	21,384.00	4.5°	-0.19	2.52 + 07	D+		
1310.5444	22,246.64	0.5°	29,874.97	1.5	-0.92	4.68 + 06	D		
1321.7602	18,310.92	5.5	25,874.52	5.5°	-0.53	1.12 + 07	D		
1322.6731	21,943.80	3.5	29,502.18	2.5°	-0.91	4.69 + 06	D		
1323.9928	12,787.404	2.5	20,338.25	2.5°	-0.60	9.62 + 06	D		
1328.5602	13,238.323	3.5	20,763.21	3.5°	-0.40	1.49 + 07	D+		
1465.8062	24,088.54	3.5°	30,908.86	2.5	-0.59	7.89 + 06	D		
1475.9447	18,315.88	4.5	25,089.35	4.5°	-0.80	4.82 + 06	D		
1486.3792	25,414.63	2.5	32,140.55	3.5°	-0.84	4.33 + 06	D		
1517.4482	23,466.84	4.5°	30,055.05	3.5	-0.90	3.64 + 06	D		
1572.4612	23,221.10	3.5°	29,578.82	2.5	-0.64	6.16 + 06	D		
1611.4542	17,099.38	2.5	23,303.26	3.5°	-0.70	5.14 + 06	D		
1624.8588	24,249.00	4.5°	30,401.70	3.5	-0.50	7.92 + 06	D+		
1640.6878	24,841.42	5.5°	30,934.76	4.5	-0.36	1.07 + 07	D+		
1647.2380	16,735.14	1.5	22,804.25	2.5°	-0.96	2.66 + 06	D		
1666.4281	21,969.32	2.5	27,968.54	1.5°	-0.96	2.62 + 06	D		
1686.7932	25,997.17	4.5°	31,923.96	4.5	-0.62	5.57 + 06	D		
1689.1713	25,558.80	1.5	31,477.22	2.5°	-0.83	3.48 + 06	D		
1760.2624	25,380.27	3.5°	31,059.69	3.5	-0.82	3.27 + 06	D		
1889.6931	25,997.17	4.5°	31,287.59	3.5	-0.89	2.40 + 06	D		
2321.1898	17,140.90	4.5	21,447.86	3.5°	-0.55	3.50 + 06	D+		
2515.1319	18,310.92	5.5	22,285.77	4.5°	-0.42	4.05 + 06	C+		
2531.7177	17,023.36	3.5	20,972.17	2.5°	-1.00	1.04 + 06	D		
2906.0572	27,619.54	4.5°	31,059.69	3.5	-0.95	8.95 + 05	D		
2987.2656	18,315.88	4.5	21,662.51	3.5°	-0.93	8.68 + 05	D		
3143.0848	28,743.24	5.5°	31,923.96	4.5	-0.54	1.96 + 06	C+		
3365.4959	28,089.17	4.5°	31,059.69	3.5	-0.82	8.99 + 05	D+		
4080.4865	27,455.31	3.5°	29,905.33	2.5	-0.94	4.59 + 05	D+		
4472.6128	29,905.33	2.5	32,140.55	3.5°	-0.97	3.57 + 05	D+		
7842.7216	30,650.28	4.5°	31,925.00	3.5	-0.86	1.48 + 05	C+		

<sup>a</sup> Air wavelengths deduced from the experimental energy levels. The conversion from vacuum to air wavelengths was obtained using the Edlén formula [35]; <sup>b</sup> Experimental energy levels from [6]. and o stands for even and odd parities, respectively; <sup>c</sup> Calculated data from the HFR+CPOL2 model (see text). The letter  $g$  stands for the statistical weight ( $2J + 1$ ) of the lower or the upper level for  $\log gf$  and  $gA$ , respectively. The estimated uncertainties are indicated by the same code letter as the one used in the NIST database [6], i.e., C+ ( $\leq 18\%$ ), C ( $\leq 25\%$ ), D+ ( $\leq 40\%$ ), D ( $\leq 50\%$ ) and E ( $> 50\%$ ) (see text); <sup>d</sup> Experimental data from [22].

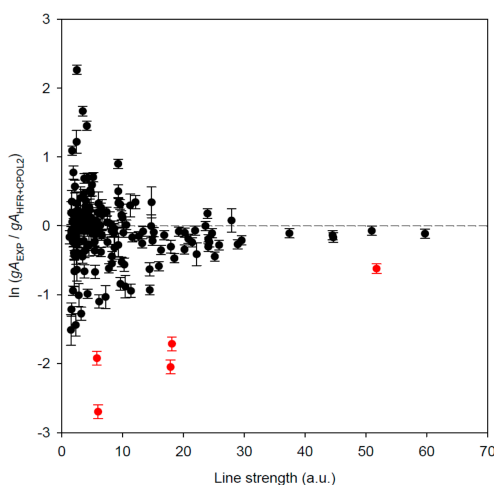


**Figure 6.** Dependence of residuals (experiment-theory) on the line strength  $S$  (in atomic units) calculated in this work. The experimental  $gA$ -values ( $gA_{EXP}$ ), together with their error bars, originate from Den Hartog et al. [22] The red outlying points have been excluded from uncertainty evaluation (see text).

In summary, the oscillator strengths and transition probabilities computed in the present work using the HFR+CPOL2 model are expected to be accurate to within a factor of two for the vast majority of the La I spectral lines listed in Table 2 and even better than 30% for many of them. These new parameters thus represent the most reliable set of theoretical radiative rates produced up until now in lanthanum atom and can be considered as a valuable complement to the available experimental data [22], in particular in the infrared region where the latter are very sparse.

#### 4. Conclusions

New oscillator strengths and transition probabilities for 392 spectral lines of neutral lanthanum are reported in this work. They were deduced from moderately large-scale pseudo-relativistic Hartree–Fock (HFR) calculations including the most important intravalence and core-valence configuration interaction effects. The accuracy of the results was estimated to be better than a factor of two for the entire set of transitions and likely within 30% for many of them. This was assessed from detailed comparisons between different theoretical models based on the HFR and the multiconfiguration Dirac–Hartree–Fock (MCDHF) methods, on the one hand, and between the theoretical results and the available experimental data, on the other hand. Among the La I lines listed in the present paper, about 60% have  $gf$ - and  $gA$ -values determined for the first time.

**Author Contributions:** All authors were equally involved in the calculations reported in the present paper as well as in the writing of the manuscript.

**Funding:** This research received no external funding.

**Acknowledgments:** P.P. and P.Q. are respectively Research Associate and Research Director of the Belgian National Fund for Scientific Research F.R.S.-FNRS. Financial support from this organization is acknowledged.

**Conflicts of Interest:** The authors declare no conflict of interest.

#### References

1. Biéumont, E.; Quinet, P. Recent Advances in the Study of Lanthanide Atoms and Ions. *Phys. Scr.* **2003**, *105*, 38. [CrossRef]
2. Wybourne, B.G. The fascination of the rare earths—Then, now and in the future. *J. Alloys Compd.* **2004**, *380*, 96–100. [CrossRef]
3. Lawler, J.E.; Den Hartog, E.A.; Sneden, C. Spectroscopic Data for Neutral and Ionized Rare Earth Elements. *AIP Conf. Proc.* **2005**, *771*, 152–161.
4. Sneden, C.; Lawler, J.E.; Cowan, J.J.; Ivans, I.I.; Den Hartog, E.A. New Rare Earth Element Abundance Distributions for the Sun and Five r-process-rich Very Metal-Poor Stars. *Astrophys. J. Suppl.* **2009**, *182*, 80. [CrossRef]
5. Mumpower, M.R.; McLaughlin, G.C.; Surman, R. The Rare Earth Peak: An Overlooked r-process Diagnostic. *Astrophys. J.* **2012**, *752*, 117. [CrossRef]
6. Kramida, A.; Ralchenko, Y.; Reader, J.; NIST ASD Team. *NIST Atomic Spectra Database*; National Institute of Standards and Technology: Gaithersburg, MD, USA, 2018. Available online: <http://physics.nist.gov/asd> (accessed on 30 October 2018).
7. Corliss, C.H.; Bozman, W.R. Experimental transition probabilities for spectral lines of seventy elements. *Nat. Bur. Stand. Monogr.* **1962**, *53*, 80–81.
8. Kurucz, R.L. Including All the Lines. *Can. J. Phys.* **2011**, *89*, 417. [CrossRef]
9. Hese, A. Level Crossing Experiments to Investigate the Hyperfine Structure and the Lifetime of the  $5d6s6p\ z\ ^2F_{5/2,7/2}$  States in the Lanthanum I Spectrum. *Z. Phys.* **1970**, *236*, 42. [CrossRef]
10. Hese, A.; Buldt, G. Hyperfine Structure, Stark Effect and Lifetimes of the Excited  $5d6s6p\ y\ ^2D_{3/2,5/2}$  States of the Lanthanum I Spectrum. *Z. Naturforsch.* **1970**, *25*, 1537–1545.
11. Hese, A.; Wiese, H.P. Investigation of the  $5d6s6p\ z\ ^2F$  Terms in the Lanthanum I Spectrum by Optical Double Resonance. *Z. Angew. Phys.* **1970**, *30*, 170.
12. Bulos, B.R.; Glassman, A.J.; Gupta, R.; Moe, G.W. Measurement of the Lifetimes of the  $z\ ^2F_{5/2}$ ,  $z\ ^2D_{3/2}$ ,  $z\ ^4G_{5/2}$ , and  $y\ ^2D_{3/2}$  States of Lanthanum. *J. Opt. Soc. Am.* **1978**, *68*, 842–845. [CrossRef]

13. Penkin, N.P.; Gorshkov, V.N.; Komarovskii, V.A. Radiative lifetimes of excited La I levels. *Opt. Spectrosc.* **1985**, *58*, 840–841.
14. Biémont, E.; Quinet, P.; Svanberg, S.; Xu, H.L. Lifetime measurements and calculations in La I. *Eur. Phys. J. D.* **2004**, *30*, 157–162. [[CrossRef](#)]
15. Karaçoban, B.; Özdemir, L. Energies and Lifetimes for Some Excited Levels in La I. *Acta Phys. Pol. A* **2008**, *113*, 1609–1618. [[CrossRef](#)]
16. Karaçoban, B.; Özdemir, L. Electric Dipole Transitions for La I ( $Z = 57$ ). *J. Quant. Spectrosc. Rad. Transf.* **2008**, *109*, 1968–1985. [[CrossRef](#)]
17. Froese-Fischer, C.F.; Brage, T.; Jönsson, P. *Computational Atomic Structure—An MCHF Approach*; Institute of Physics Publishing: Bristol, UK, 1997.
18. Feng, Y.Y.; Zhang, W.; Kuang, B.; Ning, L.; Jiang, Z.; Dai, Z. Radiative Lifetime Measurements on Odd-Parity Levels of La I by Time-Resolved Laser Spectroscopy. *J. Opt. Soc. Am. B* **2011**, *28*, 543–546. [[CrossRef](#)]
19. Feng, Y.Y.; Wang, Q.; Jiang, L.Y.; Jiang, Z.K.; Dai, Z. Radiative Lifetimes of Highly Excited Odd-Parity Levels of Neutral Lanthanum. *Eur. Phys. J. D* **2011**, *65*, 299–302. [[CrossRef](#)]
20. Yarlagadda, S.; Mukund, S.; Nakhate, S.G. Radiative lifetime measurements in neutral lanthanum using time-resolved laser-induced fluorescence spectroscopy in supersonic free-jet. *J. Opt. Soc. Am. B* **2011**, *28*, 1928–1933. [[CrossRef](#)]
21. Shang, X.; Tian, Y.; Wang, Q.; Fan, S.; Bai, W.; Dai, Z. Radiative lifetime measurements of some La I and La II levels by time-resolved laser spectroscopy. *Mon. Not. R. Astron. Soc.* **2014**, *442*, 138–141. [[CrossRef](#)]
22. Den Hartog, E.A.; Palmer, A.J.; Lawler, J.E. Radiative lifetimes and transition probabilities of neutral lanthanum. *J. Phys. B At. Mol. Opt. Phys.* **2015**, *48*, 155001. [[CrossRef](#)]
23. Cowan, R.D. *The Theory of Atomic Structure and Spectra*; University of California Press: Berkeley, CA, USA, 1981.
24. Quinet, P.; Palmeri, P.; Biémont, E.; McCurdy, M.M.; Rieger, G.; Pinnington, E.H.; Wickliffe, M.E.; Lawler, J.E. Experimental and theoretical lifetimes, branching fractions and oscillator strengths in Lu II. *Mon. Not. R. Astron. Soc.* **1999**, *307*, 934–940. [[CrossRef](#)]
25. Quinet, P.; Palmeri, P.; Biémont, E.; Li, Z.S.; Zhang, Z.G.; Svanberg, S. Radiative lifetime measurements and transition probability calculations in lanthanide ions. *J. Alloys Comp.* **2002**, *344*, 255–259. [[CrossRef](#)]
26. Quinet, P. An overview of the recent advances performed in the study of atomic structures and radiative processes in the lowest ionization stages of heavy elements. *Can. J. Phys* **2017**, in press. [[CrossRef](#)]
27. Fraga, S.; Karwowski, J.; Saxena, K.M.S. *Handbook of Atomic Data*; Elsevier: Amsterdam, The Netherlands, 1976.
28. Hibbert, A. Transitions in the Cadmium Sequence. *Nucl. Instrum. Methods Phys. Res.* **1982**, *202*, 323–327. [[CrossRef](#)]
29. Hameed, S. Core Polarization Corrections to Oscillator Strengths and Singlet-Triplet Splittings in Alkaline Earth Atoms. *J. Phys. B* **1972**, *5*, 746. [[CrossRef](#)]
30. Başar, G.; Gamper, B.; Güzelçimen, F.; Öztürk, I.K.; Binder, T.; Başar, G.; Kröger, S.; Windholz, L. New Even and Odd Parity Fine Structure Levels of La I Discovered by Means of Laser-Induced Fluorescence Spectroscopy. *J. Quant. Spectrosc. Rad. Transfer.* **2017**, *187*, 505–510. [[CrossRef](#)]
31. Jönsson, P.; Gaigalas, G.; Bieron, J.; Froese Fischer, C.; Grant, I.P. New Version: GRASP2K Relativistic Atomic Structure Package. *Comput. Phys. Commun.* **2013**, *184*, 2197–2203. [[CrossRef](#)]
32. Grant, I.P. *Relativistic Quantum Theory of Atoms and Molecules. Theory and Computation*; Springer: New York, NY, USA, 2007.
33. Zhang, W.; Palmeri, P.; Quinet, P.; Biémont, E. Transition probabilities in Te II and Te III spectra. *Astron. Astrophys.* **2013**, *551*, A136. [[CrossRef](#)]
34. Kramida, A. Critical evaluation of data on atomic energy levels, wavelengths, and transition probabilities. *Fusion Sci. Technol.* **2013**, *63*, 313–323. [[CrossRef](#)]
35. Edlén, B. The refractive index of air. *Metrologia* **1966**, *2*, 71. [[CrossRef](#)]

